

# Developing Cathode Materials for Aqueous Zinc Ion Batteries: Challenges and Practical Prospects

Guanjie Li, Liang Sun, Shilin Zhang,\* Chaofeng Zhang, Huanyu Jin, Kenneth Davey, Gemeng Liang, Sailin Liu, Jianfeng Mao, and Zaiping Guo\*

Growth in intermittent renewable sources including solar and wind has sparked increasing interest in electrical energy storage. Grid-scale energy storage integrated with renewable sources has significant advantages in energy regulation and grid security. Aqueous zinc-ion batteries (AZIBs) have emerged as a practically attractive option for electrical storage because of environmentally benign aqueous-based electrolytes, high theoretical capacity of Zn anode, and significant global reserves of Zn. However, application of AZIBs at the grid-scale is restricted by drawbacks in cathode material(s). Herein, a comprehensive summary of the features and storage mechanisms of the latest cathode materials is provided. The fundamental problems and corresponding in-depth causes for cathode materials is critically reviewed. It is also assess practical challenges, appraise their translation to commerce and industry, and systematically summarize and discuss the potential solutions reported in recent works. It is established necessary design strategies for Zn anodes and electrolytes that are matched with cathode materials for commercializing AZIBs. Finally, it is concluded with a perspective on the practical prospects for advancing the development of future AZIBs. Findings will be of interest and benefit to a range of researchers and manufacturers in the design and application of AZIBs for grid-scale energy storage.

## 1. Introduction


The concentration of carbon dioxide (CO<sub>2</sub>) in the atmosphere reportedly reached 419 ppm in Oct 2022.<sup>[1]</sup> This adds to warming the planet and is important in climate change. Increasing CO<sub>2</sub> has catalyzed a rapid global growth in renewable energy, including solar and wind.<sup>[2]</sup> Renewable electricity capacity is reportedly forecast to increase by > 60% between 2020 and 2026, reaching more than 4800 GW.<sup>[3]</sup> Battery-based energy storage is seen as important to enabling renewable, intermittent energy sources. Because of a relatively favorable energy density, lithium-ion batteries (LIBs) with organic electrolyte(s) are practically attractive for portable electronics and electric vehicles, however large scale production is limited by finite (low) lithium reserves, high (and fluctuating) cost and safety risks that restrict grid-scale application.

Rechargeable aqueous zinc ion batteries (AZIBs) are, especially, practically promising for grid-scale energy storage because of abundant Zn, low cost, high ionic conductivity and reduced safety risks.<sup>[4]</sup> The use of Zn electrodes in batteries is not new. Primary Zn batteries including Zn-air, Zn//NiOOH, Zn//Ag<sub>2</sub>O and Zn//MnO<sub>2</sub> are reportedly globally available, in which Zn//MnO<sub>2</sub> is dominant.<sup>[5]</sup> Initial attempts to develop rechargeable AZIBs were reportedly hindered by limited chemical and electrochemical compatibility between electrolyte and Zn electrodes, such as a narrow working voltage window, poor reversible Zn plating/stripping, and low Coulombic efficiency (CE) due to formation of Zn dendrites and irreversible byproducts (e.g., ZnO and Zn(OH)<sub>2</sub>) in alkaline environment(s).<sup>[6]</sup> The limitations associated with alkaline electrolytes have driven research interest in alternatives including mildly acidic and neutral electrolytes. The adoption of these “new” electrolyte systems has enabled the successful development of rechargeable AZIBs, such as Zn// $\alpha$ -MnO<sub>2</sub> cells.<sup>[7]</sup> Continuing research on AZIBs chemistries has concentrated on protection of metallic Zn anodes, development of cathode materials, together with exploration of compatible electrolyte(s) and novel separator(s).<sup>[8]</sup>

The particular electrochemistry of Zn imposes nontrivial limitations on cathode materials including, being stable at high voltage and concurrently exhibiting large capacity. Similar to

G. Li, L. Sun, S. Zhang, H. Jin, K. Davey, G. Liang, S. Liu, J. Mao, Z. Guo  
School of Chemical Engineering and Advanced Materials  
Faculty of Sciences, Engineering and Technology  
The University of Adelaide  
Adelaide, SA 5005, Australia  
E-mail: shilin.zhang01@adelaide.edu.au; zaiping.guo@adelaide.edu.au

C. Zhang  
Institutes of Physical Science and Information Technology  
Leibniz Joint Research Center of Materials Sciences  
Engineering Laboratory of High-Performance Waterborne Polymer  
Materials of Anhui Province  
Anhui Graphene Engineering Laboratory  
Key Laboratory of Structure and Functional Regulation of Hybrid  
Material (Ministry of Education)  
Anhui University  
Hefei 230601, China

 The ORCID identification number(s) for the author(s) of this article can be found under <https://doi.org/10.1002/adfm.202301291>.

© 2023 The Authors. Advanced Functional Materials published by Wiley-VCH GmbH. This is an open access article under the terms of the Creative Commons Attribution-NonCommercial License, which permits use, distribution and reproduction in any medium, provided the original work is properly cited and is not used for commercial purposes.

DOI: 10.1002/adfm.202301291

LIBs, the selection of cathode materials largely determines cost of AZIBs and electrochemical performance. With Zn metal as anode, the open circuit voltage (OCV) and capacity for an AZIB are determined by selection of the cathode material.<sup>[9]</sup> Significant rate performance and gravimetric power density is exhibited only if Zn-insertion cathode materials yield high ionic/electronic transport and sufficient redox reaction kinetics in the cathode and, at cathode–electrolyte interface(s). It is acknowledged that good cycling stability with AZIBs will be dependent on structural integrity and stability of cathode materials. Over the recent 10 years there has been a research focus on cathode materials compatible with highly reversible Zn intercalation/de-intercalation, with use of Prussian blue analogues, vanadium-based materials, Chevrel phase compounds and organic compounds. However, these materials do not exhibit sufficient electrochemical performance, making them less attractive for commercialization in rechargeable AZIBs. Importantly however, despite reports of cathodes with demonstrated large reversible capacity at high voltage, findings from most reports were not transferable to practical devices because of difficulty in rigorous interpretation of performance, highlighting a need for more agreed and systematic methods with cathode materials.

In this Review, we provide a comprehensive summary of the features and storage mechanisms of the latest cathode materials. We critically review the fundamental problems and corresponding in-depth causes for cathode materials. We also assess

practical challenges, appraise their translation to commerce and industry, and systematically summarize and discuss the potential solutions reported in recent works. We establish necessary design strategies for Zn anodes and electrolytes that are matched with cathode materials for commercializing AZIBs. Finally, we conclude with a perspective on the practical prospects for advancing the development of future AZIBs. Findings will be of interest and benefit to a range of researchers, engineers and manufacturers of equipment in understanding and applying AZIBs for grid-scale energy storage.

## 2. Research Progress and Practical Challenges

### 2.1. Electrochemical Mechanism for Zn<sup>2+</sup> Ion Storage

Development of AZIBs is predicated on selection of cathode material(s) that, generally can be divided into Mn-, and V-, based materials, Prussian Blue Analogues (PBAs), organic compounds, layered chalcogenides, other metal oxides and polyanions, together with conversion-type materials. Cathode materials are of research interest for mild-acid AZIBs because of practical potential for grid-scale energy storage. Understanding Zn storage mechanism(s) therefore is important to rational design of cathode materials for improved electrochemical performance. As presented in **Figure 1**, there are six (6) storage

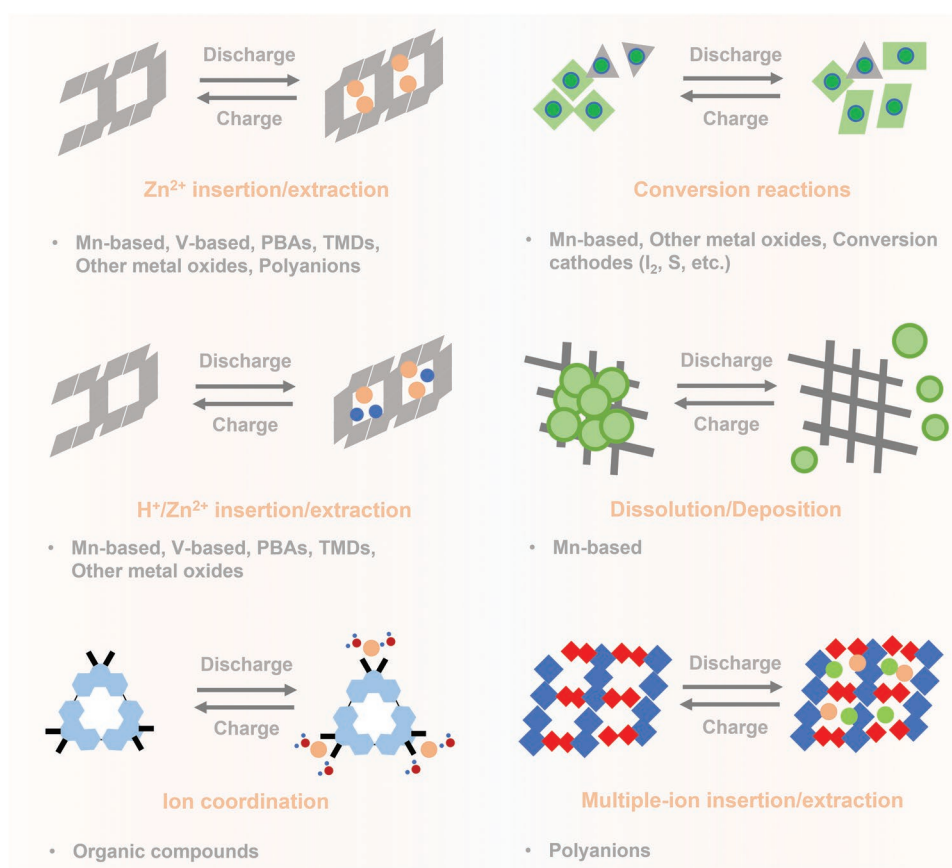


**Figure 1.** Schematic diagrams of the storage mechanism for representative cathode materials for AZIBs.

mechanisms for cathode materials, 1)  $\text{Zn}^{2+}$  insertion/extraction, 2) conversion reactions, 3)  $\text{H}^+/\text{Zn}^{2+}$  insertion/extraction, 4)  $\text{Mn}^{2+}/\text{MnO}_2$  dissolution/deposition, 5) ion coordination, and 6) multiple-ion insertion/extraction. Representative chemical equations are given in Table 1.

### 2.1.1. Mn-Based Cathodes

Manganese (Mn)-based oxides, including  $\text{MnO}_2$  polymorphs ( $\alpha$ -,  $\beta$ -,  $\gamma$ -,  $\epsilon$ -,  $\delta$ -, and todorokite- $\text{MnO}_2$ ),  $\text{Mn}_2\text{O}_3$ ,  $\text{Mn}_3\text{O}_4$ ,  $\text{MnO}$  and  $\text{ZnMn}_2\text{O}_4$ , are reportedly used as cathodes for energy storage and conversion because of abundance, relatively low toxicity and capacity.<sup>[10]</sup> These advantages make manganese materials most popular as cathodes for AZIBs. As an example, theoretical specific capacity for  $\text{MnO}_2$  is 308 mA h  $\text{g}^{-1}$  based on discharge product of  $\text{Zn}_{0.5}\text{MnO}_2$  and, mean discharge plateau is 1.2 to 1.4 V for  $\text{Zn}/\text{MnO}_2$  cell.<sup>[11]</sup>

Despite significant progress, Mn-based cathodes however usually exhibit rapid capacity fading on cycling and poor rate performance. Additionally, there is no agreement on the  $\text{Zn}^{2+}$  ion storage mechanism(s). Four(4) storage mechanisms have been reported for  $\alpha$ - $\text{MnO}_2$ , namely, 1) reversible Zn ion insertion/extraction into/from bulk cathodes, which involves a reversible phase transformation from  $\text{MnO}_2$  to products with layered or spinel structures, 2) chemical conversion reaction between  $\alpha$ - $\text{MnO}_2$  and  $\text{H}^+$ , 3) the uptake/removal of both  $\text{Zn}^{2+}$  and  $\text{H}^+$  at different charge/discharge stages, and 4)  $\text{Mn}^{2+}/\text{MnO}_2$  dissolution-deposition.<sup>[11b,12]</sup> There is little reported agreement on electrochemical storage mechanism(s) for Mn-based materials, evidencing a need for systematic determinations based on the crystallographic structure, particle morphology and pH value of electrolytes.

### 2.1.2. V-Based Cathodes

Vanadium oxides are widely reported as cathode materials for AZIBs because the vanadium oxidation states ( $\text{V}^{x+}$  ( $x = 2, 3, 4, 5$ )) and redox properties are various. Basic V–O coordination polyhedra are assembled into different frameworks of vanadium oxides, whereas the V coordination polyhedra varies from tetrahedron through square pyramid and trigonal bipyramid, to distorted and regular octahedra. These continuous changes in both complex polyhedra and V oxidation can be practically adjusted to accommodate  $\text{Zn}^{2+}$  ions to produce “good” electrochemical performance. The conventional mechanism for V-based AZIBs is insertion/extraction of  $\text{Zn}^{2+}$  in the selected host material(s), while the  $\text{Zn}^{2+}$  transfer, ion-insertion thermodynamics and kinetics are reportedly improved with  $\text{H}^+$  ions. The ion-insertion sequence and transfer kinetics depend on structure of cathode materials, crystallographic polymorphs and particle size of active materials.<sup>[13]</sup> The  $\text{H}^+/\text{Zn}^{2+}$  co-intercalation mechanism is not understood, with unknowns including, position of inserted  $\text{H}^+$  ions in cathodes and how the  $\text{H}^+$  insertion affects the insertion of  $\text{Zn}^{2+}$  ions. Additionally, the two (2) mechanisms are reportedly classified as reversible cationic redox reactions, while the oxygen redox reaction with relatively greater potential, is activated if both suitable cathode material(s) and electrolyte(s) are selected. The oxygen activity needs to be

boosted to achieve an anion redox reaction; one method is to increase the electron density of oxygen.<sup>[13,14]</sup>

### 2.1.3. PBAs-Based Cathodes

PBAs are attractive for use in battery systems including,  $\text{Li}^+$ ,  $\text{Na}^+$ ,  $\text{K}^+$  and  $\text{Zn}^{2+}$ , and grid-scale applications because of “large” open structures robust structural stability, versatile ion-storage capability and sufficient redox-active sites.<sup>[15]</sup>

The generic formulation for a PBA component can be represented as  $\text{A}_x\text{M}_1[\text{M}_2(\text{CN})_6]_y \cdot n\text{H}_2\text{O}$  ( $0 \leq x \leq 2$ ;  $y \leq 1$ ), where A represents alkaline, and M transition metals.<sup>[16]</sup> PBAs have an open 3D structure with “large” storage sites in which  $\text{Zn}^{2+}$  ions reversibly “shuttle”. Because of high operating voltage of AZIBs with the PBAs cathode of 1.5 to 1.8 V, cells exhibit specific energy density from 100 to 120 Wh  $\text{kg}^{-1}$ , based on total mass of active electrode materials.<sup>[10a]</sup> Typically, both vacancies and crystal water exist in the structure of the PBAs because of rapid precipitation and are the important factors influencing performance of PBAs for AZIBs, i.e., cycling stability. For storage mechanism for PBAs, the reversible  $\text{Zn}^{2+}$  ion intercalation/de-intercalation reaction is most common, however  $\text{Zn}^{2+}/\text{H}^+$  intercalation/de-intercalation is also observed in some PBAs including, vanadium hexacyanoferrate PBA.<sup>[17]</sup> Additionally, the number of vacancies and crystal water in PBAs affects storage mechanism(s). The effect of non-ferrous metal ions, especially electrochemically active metals, Mn, Co and V, on the charge storage behaviors of PBA materials needs future assessment.

### 2.1.4. Organic-Based Cathodes

Organic compounds, including molecules and polymers, are attractive because of environmental friendliness, sustainability, low cost, tuneable structure and fast reaction kinetics.<sup>[10a,18]</sup> Based on electrochemically active groups and redox chemistry, organic electrode materials (OEMs) can be classified into three (3) categories: 1) *n*-type, materials based on C=O bond reaction (carbonyl active materials) and C=N bond reaction, 2) *p*-type, triphenylamine derivatives, organosulfur polymers and nitroxide radical-based polymers, and 3) bipolar types, conducting polymers. In contrast to traditional intercalation/de-intercalation mechanism for inorganic host species in AZIBs, the storage mechanism for conjugated carbonyl materials is a reversible heterogeneous enolization coupled with ion-coordination reaction.<sup>[19]</sup> For example, the *p*-type cathode during charging loses electrons and converts to a positively charged state ( $\text{P}^+$ ), coordinating with anions from electrolytes to maintain molecule neutrality. In contrast, *n*-type cathodes are changed from a negatively charged state ( $\text{N}^-$ ) to a neutral state, together with release of coordinated cations to electrolytes. Bipolar organic electrodes can be converted to a positively charged state ( $\text{P}^+$ ) when losing electrons, or to a negatively charged state ( $\text{N}^-$ ) when gaining electrons. In addition to the charge carrier,  $\text{H}^+$  can also be the phase transfer mediator in Zn-organic batteries including,  $\text{Zn}/p$ -chloranil cells.<sup>[19]</sup> It is therefore important for organic-based cathodes to confirm the function of protons in aqueous electrolytes.

**Table 1.** Comparative summary of mechanisms for representative cathodes in AZIBs.

Cathodes	Cathode reaction	Mechanism
Mn-based		
MnO <sub>2</sub> <sup>[34]</sup>	$2\text{MnO}_2 + \text{Zn}^{2+} + 2\text{e}^- \leftrightarrow \text{ZnMn}_2\text{O}_4$	Zn <sup>2+</sup> insertion/extraction
MnO <sub>2</sub> <sup>[35]</sup>	$\text{MnO}_2 + \text{H}^+ + \text{e}^- \leftrightarrow \text{MnOOH}$ $3\text{Zn}^{2+} + 6\text{OH}^- + \text{ZnSO}_4 + \text{xH}_2\text{O} \leftrightarrow \text{ZnSO}_4 [\text{Zn}(\text{OH})_2]_3 \text{xH}_2\text{O}$	Conversion
MnO <sub>2</sub> <sup>[11b]</sup>	$\text{MnO}_2 + \text{H}^+ + \text{e}^- \leftrightarrow \text{MnOOH}$ $\text{Zn}^{2+} + 2\text{e}^- + 2\alpha\text{-MnO}_2 \leftrightarrow \text{ZnMn}_2\text{O}_4$	H <sup>+</sup> /Zn <sup>2+</sup> insertion/extraction
MnO <sub>2</sub> <sup>[36]</sup>	$\text{MnO}_2 + \text{H}^+ + 2\text{e}^- \leftrightarrow \text{Mn}^{2+} + 2\text{H}_2\text{O}$	Dissolution/deposition
V-based		
Zn <sub>0.25</sub> V <sub>2</sub> O <sub>5</sub> ·nH <sub>2</sub> O <sup>[37]</sup>	$\text{Zn}_{0.25}\text{V}_2\text{O}_5 \cdot \text{nH}_2\text{O} + 1.1\text{Zn}^{2+} + 2.2\text{e}^- \leftrightarrow \text{Zn}_{1.35}\text{V}_2\text{O}_5 \cdot \text{nH}_2\text{O}$	Zn <sup>2+</sup> insertion/extraction
NaV <sub>3</sub> O <sub>8</sub> ·1.5H <sub>2</sub> O <sup>[38]</sup>	$3.9\text{H}_2\text{O} \leftrightarrow 3.9\text{H}^+ + 3.9\text{OH}^-$ $\text{NaV}_3\text{O}_8 \cdot 1.5\text{H}_2\text{O} + 3.9\text{H}^+ + 0.5\text{Zn}^{2+} + 4.9\text{e}^- \rightarrow \text{H}_{3.9}\text{NaZn}_{0.5}\text{V}_3\text{O}_8 \cdot 1.5\text{H}_2\text{O}$	H <sup>+</sup> /Zn <sup>2+</sup> insertion/extraction
PBAs		
Zn hexacyanoferrate <sup>[17b]</sup>	$\text{xZn}^{2+} + 2\text{x}\text{e}^- + \text{Zn}_3[\text{Fe}(\text{CN})_6]_2 \leftrightarrow \text{Zn}_{3+\text{x}}[\text{Fe}(\text{CN})_6]_2$	Zn <sup>2+</sup> insertion/extraction
VO hexacyanoferrate <sup>[17d]</sup>	$(\text{VO})_{1.31}\text{Fe}(\text{CN})_6 \cdot 5.95\text{H}_2\text{O} + \text{xZn}^{2+} + 2\text{x}\text{e}^- \leftrightarrow \text{Zn}_\text{x}(\text{VO})_{1.31}\text{Fe}(\text{CN})_6 \cdot 5.95\text{H}_2\text{O}$	H <sup>+</sup> /Zn <sup>2+</sup> insertion/extraction
Organics		
Triangular phenanthrenequinone-based macrocycle (PQ-Δ) <sup>[39]</sup>	$\text{PQ-}\Delta + 3\text{Zn}(\text{CF}_3\text{SO}_3)_2 + \text{xH}_2\text{O} + 6\text{e}^- \leftrightarrow \text{PQ-}\Delta \cdot 3\text{Zn}^{2+} \cdot \text{xH}_2\text{O} + 6(\text{CF}_3\text{SO}_3)_2^-$	Ion-coordination
TMDs		
MoS <sub>2</sub> <sup>[40]</sup>	$\text{xZn}^{2+} + \text{x}\text{e}^- + \text{MoS}_2 \leftrightarrow \text{Zn}_\text{x}\text{MoS}_2$	Zn <sup>2+</sup> insertion/extraction
Other metal oxides		
MnO <sub>x</sub> <sup>[26a]</sup>	$\text{MoO}_\text{x} + \text{yZn}^{2+} + 2\text{y}\text{e}^- \rightleftharpoons \text{Zn}_\text{y}\text{MoO}_\text{x}$	Zn <sup>2+</sup> insertion/extraction
CuO <sup>[25c]</sup>	$3\text{CuO} + 4\text{H}^+ + 4\text{e}^- \rightarrow \text{Cu} + \text{Cu}_2\text{O} + 2\text{H}_2\text{O}$ (first charge) $\text{Cu}_2\text{O} + 2\text{H}^+ + 2\text{e}^- \leftrightarrow 2\text{Cu} + \text{H}_2\text{O}$ (following cycles)	Conversion
Polyanion		
VOPO <sub>4</sub> <sup>[30]</sup>	$\text{VO}^{y+}\text{PO}_4 + \text{xZn}^{2+} + (2\text{x} + \text{y})\text{e}^- \leftrightarrow \text{Zn}_\text{x}\text{VOPO}_4$	Zn <sup>2+</sup> insertion/extraction
Na <sub>3</sub> V <sub>2</sub> (PO <sub>4</sub> ) <sub>3</sub> <sup>[29a]</sup>	$\text{Na}_3\text{V}_2(\text{PO}_4)_3 \rightarrow (3\text{-x})\text{Na}^+ + (3\text{-x})\text{e}^- + \text{Na}_\text{x}\text{V}_2(\text{PO}_4)_3$ (first charge) $\text{Na}_\text{x}\text{V}_2(\text{PO}_4)_3 + \text{zZn}^{2+} + \text{yNa}^+ + (2\text{z} + \text{y})\text{e}^- \leftrightarrow \text{Zn}_\text{z}\text{Na}_{(\text{x} + \text{y})}\text{V}_2(\text{PO}_4)_3$ (following cycles)	Multi-ion insertion/extraction
Conversion Cathodes		
I <sub>2</sub> <sup>[33]</sup>	$\text{I}_2 + 2\text{e}^- \leftrightarrow 2\text{I}^-$	Conversion
S <sup>[41]</sup>	$\text{S} + \text{Zn}^{2+} + 2\text{e}^- \leftrightarrow \text{ZnS}$	Conversion

In addition to organic species, research interests have focused on metal-organic frameworks (MOFs) and covalent organic frameworks (COFs) because of the ordered and functional porosities with “large” surface areas that boost ion transport and transfer kinetics.<sup>[20]</sup> MOFs and COFs composed of selected electrochemically active transition metals, or organic linkers, share similarities, enabling flexible structural design engineering, optimizing platform voltage, charge transfer and integral flexibility. Currently reported MOFs that contain hydroxy and carbonyl groups as ligand and redox couples in MOFs, reportedly exhibit reversible metal-ion deintercalation/intercalation properties in AZIBs.<sup>[21]</sup> In addition to metal-cation redox activity that can be provided by transition metals with multi-valence, e.g., V<sup>4+</sup>/V<sup>5+</sup>, Co<sup>2+</sup>/Co<sup>3+</sup>, Fe<sup>2+</sup>/Fe<sup>3+</sup>, Cu<sup>+</sup>/Cu<sup>2+</sup> and W<sup>4+</sup>/W<sup>5+</sup>, other coordination sites in MOFs, or COFs with Zn<sup>2+</sup> can be extended rather than be limited to carbonyl and hydroxy groups including, MOFs with cyano groups as ligand.<sup>[22]</sup> However, MOFs and COFs used directly as cathodes appear to be developed at slower pace than traditional organic compounds

because of structural instability and the lack of reversible sites at high potential.

### 2.1.5. Layered Transition Metal Dichalcogenides-Based Cathodes

Transition metal dichalcogenides (TMDs) are usually denoted MX<sub>2</sub>, where M is transition metal, e.g., Mo, Ti and V and, X chalcogen atoms, e.g., S, Se and Te. Among these, layered TMDs including MoS<sub>2</sub>, VS<sub>2</sub> and VSe<sub>2</sub> are reported to efficiently store Zn<sup>2+</sup> ions, based on typical Zn<sup>2+</sup> intercalation chemistry.<sup>[22,23]</sup> They exhibit a working voltage window of < 0.8 V and a specific capacity of < 250 mA h g<sup>-1</sup> that is attributed to the high Zn<sup>2+</sup> intercalation energy barrier at the electrode-electrolyte interface and the absence of H<sup>+</sup> intercalation. Despite H<sup>+</sup> intercalation being confirmed in some layered TMDs, only 10% of observed capacity reportedly comes from H<sup>+</sup> intercalation, far less than for Mn- and V-based oxides. The reason is, most likely, the formation of a strong hydrogen bond following

H<sup>+</sup> intercalations into the oxide host and weak S-H and Se-H interactions.

### 2.1.6. Other Metal Oxides-Based Cathodes

In addition to manganese and vanadium oxides, other metal oxides, such as layered MoO<sub>3</sub> and spinel Fe<sub>2</sub>O<sub>3</sub> and spinel ZnCo<sub>2</sub>O<sub>4</sub>, can also accommodate Zn<sup>2+</sup> ions. However, they generally exhibit lower conductivity and reversible specific capacity (< 200 mA h g<sup>-1</sup>) compared to manganese and vanadium oxides.<sup>[24]</sup> Nevertheless, with certain modifications, some molybdenum- and copper- oxides can achieve a reversible capacity of over 250 mA h g<sup>-1</sup>.<sup>[25]</sup> The charge storage mechanism for these materials typically relies on H<sup>+</sup>, Zn<sup>2+</sup> insertion or H<sup>+</sup>/Zn<sup>2+</sup> co-insertion, while CuO and Cu<sub>2</sub>O cathodes follow a conversion reaction mechanism.<sup>[25a,c,26]</sup> Despite their high capacity, the low discharge plateau remains a major challenge for their use in AZIBs. In addition, the relatively high cost of Mo may limit its scalability for large-scale energy storage. In contrast, exploring oxides composed of earth-abundant elements such as Fe and Cu offers an advantageous approach, and increasing their energy density is a crucial objective that deserves significant attention.

### 2.1.7. Polyanionic Compounds-Based Cathodes

Compared with other cathode materials, polyanionic compounds are attractive as cathode materials for AZIBs because of a unique covalent-bonded framework providing robust structural and thermal stability, with increased cycle life and safety. In addition, interstitial tunnels generated from the open network structure for ionic conduction, and high voltage, with the inductive effect of the polyanion and rich structural diversity, provide high flexibility for materials design.<sup>[10a,27]</sup> Typically, research with polyanions in AZIBs focuses on phosphate and fluorophosphate. Although many polyanionic compounds exhibit relatively low specific capacities because of intrinsically significant molecular mass, the strong interaction between the P-O chemical bonds in PO<sub>4</sub><sup>3-</sup> groups “unlocks” potential for use as a high-voltage cathode > 1.3 V.<sup>[28]</sup> The charge storage mechanism for polyanion cathodes involves Zn<sup>2+</sup> intercalation/de-intercalation, Na<sup>+</sup>/Zn<sup>2+</sup> intercalation/de-intercalation such as in Zn//Na<sub>3</sub>V<sub>2</sub>(PO<sub>4</sub>)<sub>3</sub> cells, or Zn<sup>2+</sup> intercalation/de-intercalation accompanied with H<sup>+</sup> intercalation/de-intercalation.<sup>[29]</sup> Highly reversible O-related redox chemistry in the high voltage region of 1.8 to 2.1 V without oxygen evolution reaction(s), was reportedly observed in layered polyanionic compounds including, VOPO<sub>4</sub> and hydrates.<sup>[30]</sup>

### 2.1.8. Other Cathodes

It is reportedly practical to increase the energy of AZIBs via replacing the storage mechanism from traditional ion intercalation to conversion-type cathodes with multiple-electron transfer. Among these, halogen materials are new materials with a conversion-type storage mechanism.<sup>[31]</sup> Compared with gaseous

chlorine and liquid bromine, there has been relatively rapid advances in aqueous Zn–I<sub>2</sub> batteries with a focus on developing I<sub>2</sub> host materials.

Typically, the energy storage mechanism relies on a single-electron conversion reaction of iodine (I<sup>-</sup>/I<sup>0</sup>) and the highly significant and necessary excess of host materials.<sup>[32]</sup> However, this is reportedly addressed via activating I<sub>2</sub> to multi-electron conversion. For example, a nearly doubling in energy density was reported in development of iodine-decorated MXene cathodes because of an additional discharging plateau assigned to I<sup>-</sup>/I<sup>+</sup> at 1.65 V versus Zn/Zn<sup>2+</sup> other than the normal plateau of 1.3 V versus Zn/Zn<sup>2+</sup>.<sup>[33]</sup> In addition, conversion-type cathodes involving multi-electron transfer reactions including, S, Se and Te, exhibit significant capacity at a relatively high potential to significantly improve energy density of AZIBs. However, these conversion-type cathodes are not widely applied because of present inferior electric conductivity, sluggish reaction kinetics of the multi-electron transfer and the solution/shuttle effect(s).

In summary, because of the diversity of cathode materials, AZIBs systems with a range of energy density have been developed. However, despite developments AZIBs do not realistically meet the energy requirements for grid-scale application(s). Fundamental mechanism(s) impact redox potential, storage capacity, charge transfer and structural stability. However, the mechanism for Zn<sup>2+</sup> ion storage in AZIBs systems is complex and is poorly understood. Improved understanding is likely to result from judiciously combined *operando* techniques and computational simulation, targeted on reaction(s) and material evolution during charge/discharge. The interactions between electrolyte, interfaces, anode and cathode should be considered.

## 2.2. Challenges for Practical Cathode Materials

In addition to poor understanding of charge storage chemistry and critical factors that control electrochemical reactivity in cathode materials, additional problems include, dissolution of active materials, side reactions, structural instability and low energy density. Poor understanding of these limits practical application of AZIBs.

### 2.2.1. Dissolution of Active Materials

The redox chemistry for cathode materials differs depending on the salt and pH value of the aqueous electrolyte. Compared with alkaline electrolytes, mild-acid aqueous electrolytes are preferable because of weak-corrosive impact and good compatibility with Zn anode. However, these can degrade the electrochemical and chemical stability of cathode materials, leading to dissolution of active materials into the electrolyte, which can be further aggravated owing to the increasing protons from the water splitting. As a result, the cathode materials undergo structural degradation/collapse, and the cell fails because of limited life span. For example, Mn-based cathodes, as can be seen in the Pourbaix diagram for manganese oxides, **Figure 2a**, MnO<sub>2</sub> will spontaneously transform to Mn<sup>2+</sup> in mild-acid electrolytes via reduction when the potential is < 0.8 V versus Standard Hydrogen Electrode (SHE).<sup>[42]</sup> Given that the redox potential for

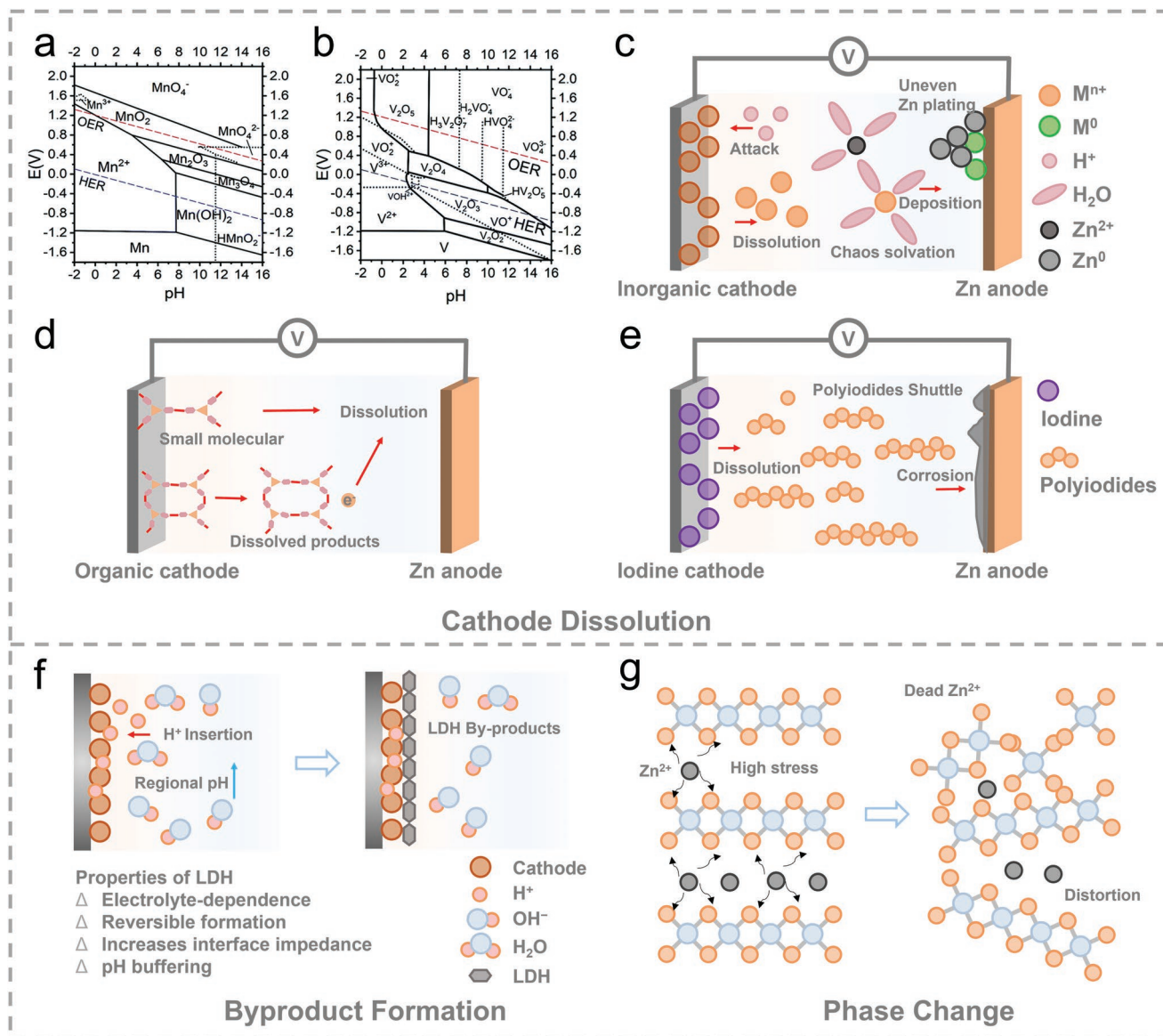


**Figure 2.** Pourbaix diagram for a) Manganese and b) Vanadium, oxides. Reproduced with permission.<sup>[42]</sup> Copyright 2019, Wiley-VCH GmbH. Schematic for dissolution of c) Inorganic, d) Organic and e) Iodine, cathodes. Schematic for f) Byproduct formation and g) Phase change.

$Zn/Zn^{2+}$  is  $-0.76$  V versus SHE,  $Mn^{2+}$  species will be generated at  $\approx 1.56$  V during discharge of  $Zn/MnO_2$  full cells. Considering the operating voltage window for  $Zn/MnO_2$  batteries ranges from 0.8 to 1.9 V, the dissolution of  $Mn^{2+}$  ions is reportedly observed during most of the state of charge. Importantly, the solubility of  $Mn^{2+}$  ions is high in water, e.g., for  $MnSO_4$ , 70 g per 100 mL of  $H_2O$  at 7 °C, that evidences a significant number of manganese ions are dissolved in the electrolyte at the end of the discharge. It has been found that the dissolved  $Mn^{2+}$  in the aqueous electrolyte occupies  $\approx 1/3$  of the total Mn in the cathode electrode following discharge.<sup>[43]</sup> Worse still, as the concentration of dissolved  $Mn^{2+}$  increases, tiny nanograins consisting of  $Zn^{2+}$  and  $Mn^{2+}$  precipitate from the electrolyte, which are unlikely to be electrochemically decomposed once deposited on the cathode surface.<sup>[44]</sup> These highly irreversible byproducts inevitably cause the permanent loss of active Mn, leading to the

capacity decay of the  $MnO_2$  cathode. It is worth noting that the formation of  $Zn^{2+}/Mn^{2+}$  nanograins is only triggered when the  $Mn^{2+}$  concentration exceeds a certain value, indicating that the dissolved  $Mn^{2+}$  can still be converted to active  $MnO_2$  in the early stage if there are adequate electric contacts and reaction sites available. As for the Zn anode, although the dissolved  $Mn^{2+}$  is unlikely to be deposited on the Zn anode as the redox potential of  $Mn/Mn^{2+}$  is  $-1.185$  V (vs. SHE), a value less than that for  $Zn/Zn^{2+}$ , it can affect the solvation environment of  $Zn^{2+}$  and the redox reaction of Zn anode. As a result, Mn-based cathodes exhibit inferior reversibility and cycling performance, despite energy densities  $> 300$  Wh  $kg^{-1}$  that are exhibited because of large capacity and high operating voltage. Additionally, the dissolution of  $Mn^{2+}$  reportedly induces phase transition from fundamental building blocks of  $MnO_6$  octahedra in  $MnO_2$  to other polymorphs as either crystalline or amorphous.

Similarly, V-based cathodes exhibit vanadium dissolution during cycling in AZIBs, especially in weakly acidic aqueous  $\text{ZnSO}_4$  and  $\text{Zn}(\text{CF}_3\text{SO}_3)_2$  because of strong polarity of water molecules and anions. The structural disintegration is increased as cycling proceeds because the coordinated water molecules and  $\text{Zn}^{2+}$  ions co-insert into the interlayer spacing/tunnel of vanadium cathodes forming the hydrogen bond with the lattice  $\text{O}^{2-}$  and weakening the V–O bond strength.

Therefore, capacity fading can be reflected from the V-based cathode cycled at low current density, but excellent cyclability is exhibited at high rates as the vanadium dissolution is inhibited. Meanwhile, the dissolution species is complex due to the multivalence of V in vanadium cathodes. As shown in Figure 2b, Boyd et al.<sup>[45]</sup> reported that the dissolution of vanadium greatly depends on the activity of  $\text{H}^+$  in the aqueous electrolyte. When the pH is < 3.0, vanadium will be presented as  $\text{VO}_2^+$  under the potential below 0.45 V (vs. SHE, 1.21 V vs.  $\text{Zn}/\text{Zn}^{2+}$ ).<sup>[46]</sup> While for mild-acid electrolytes ( $3.0 < \text{pH} < 6.0$ ), the vanadium compounds will be converted to  $\text{VOH}^{2+}$  and a lower potential is necessary for the complete conversion ( $-0.05$  V vs. SHE for pH = 3,  $-0.60$  V vs. SHE for pH = 6). If the operation potential is above 0.40 V (vs. SHE, 1.06 V vs.  $\text{Zn}/\text{Zn}^{2+}$ ),  $\text{H}_3\text{V}_2\text{O}_7^-$  will be the dominant dissolved species in mild-acid electrolytes. These findings indicate that vanadium dissolution is ubiquitous when operating in mild-acid electrolytes.<sup>[46]</sup> It is also reported that the most stable species derived from the vanadium dissolution in mild-acid electrolytes is  $\text{VO}_2(\text{OH})_2^-$ , which could react with  $\text{Zn}^{2+}$  to form  $\text{Zn}_3\text{V}_2\text{O}_7(\text{OH})_2 \cdot 2\text{H}_2\text{O}$  (ZVO).<sup>[47]</sup> The ZVO could be the only host for reversible intercalation/de-intercalation of both  $\text{Zn}^+$  and  $\text{H}^+$ . The vanadium dissolution can also diffuse to the Zn anode, where V will be reduced to  $\text{V}^{3+}$  or  $\text{V}^{4+}$  species and deposited on the Zn anode, Figure 2c, decreasing the electrochemical reaction sites and the utilization of zinc. It is widely reported that stable crystal structures are thermodynamically insoluble. Therefore, vanadium-based oxides with different polymorphs could exhibit other vanadium dissolution behavior. A systematic investigation is therefore necessary to understand the adverse impacts of vanadium dissolution and provide an in-depth mechanism understanding of the dissolved substances on the Zn anode.

In addition, the performance degradation of cathodes including PBAs, polyanionic components, and TMDs is also related to the dissolution behaviors of transition metals.<sup>[48]</sup> For example, PBAs can be divided into soluble PBAs (i.e.  $\text{KFe}[\text{Fe}(\text{CN})_6]$ ) and insoluble PB (i.e.,  $\text{Fe}_4[\text{Fe}(\text{CN})_6]_3$ ), where the excessive  $\text{K}^+$  ion is related to the solubility of PBAs in electrolytes. Other reports also found that the diffusion of  $\text{Zn}^{2+}$  and the dissolution of active substances in PBAs are closely associated with the surface orientation structure.<sup>[49]</sup> As a result, for those compounds with transition metals as building blocks in aqueous electrolytes, the dissolution problem should not be neglected and the dissolution mechanism should be understood.

Different from the inorganic cathode materials, the most important problem for small organic molecules is the possibility to dissolution in the electrolyte during cycling, Figure 2d. In addition, it is well-known that organic materials with large molecular structures are chemically stable in aqueous electrolytes and almost insoluble in water, while the ionized discharge

products are prone to be dissolved in the electrolyte, especially for organic compounds with carbonyl groups,<sup>[10a,19,50]</sup> which serves as the electrochemically active center. For example, as a dissolved species,  $\text{C4Q}^{2x-}$  is soluble in the electrolyte to react with  $\text{Zn}^{2+}$  ions through the separator, forming byproducts ( $\text{Zn}_x\text{C4Q}$ ) in the uppermost layer of the exposed Zn electrode, which leads to the capacity degradation of batteries.<sup>[51]</sup> In addition to carbonyl compounds, amine compounds with the redox of C = N groups are another promising cathode material of aqueous ZIBs. Except for the pH value of electrolytes, the spatial arrangement of the amine compounds could also affect the dissolution effect. For example, Chen et al. found that phenazine with steric hindrances constructed by adjacent H atoms is not accessible to hydrated, limiting its dissolving behavior in an aqueous solution.<sup>[51]</sup>

Compared with aforementioned cathode materials, the dissolution mechanism of halogen cathodes is more complex.<sup>[31b]</sup> Taking the conversion-type iodine-based battery as an example, Figure 2e, in contrast to the reaction pathway of  $\text{I}^- \leftrightarrow \text{I}_3^- \leftrightarrow \text{I}_2$  in the non-aqueous electrolyte, the one-step conversion process of  $\text{I}^- \leftrightarrow \text{I}_2$  without polyiodide intermediates is more favorable to most aqueous rechargeable Zn// $\text{I}_2$  batteries. If the intermediate of  $\text{I}_3^-$  formed, the utilization efficiency of iodine species would be reduced, resulting in low energy density and poor stability due to the high solubility of this intermediate in an aqueous electrolyte.<sup>[52]</sup> In addition, the liquid-liquid conversion reaction mechanism in the Zn// $\text{I}_2$  battery endows its fast kinetics and excellent rate capability, which makes it a potential candidate for liquid-flow batteries. Nevertheless, upon the continuous accumulation of  $\text{I}_2$  at the end of charge, other polyiodide species, such as  $\text{I}_5^-$ ,  $\text{I}_7^-$ , and  $\text{I}_9^-$ , will be generated.<sup>[53]</sup> These soluble species together with  $\text{I}_3^-$  will diffuse to the Zn anode under the drive of the concentration gradient, triggering the irreversible reactions between polyiodides and Zn metals and finally causing active material loss at both the cathode and the anode.<sup>[31b,53,54]</sup>

### 2.2.2. Parasitic Byproducts Formation

Continuous discharge–charge will boost the generation of unexpected byproducts. The selection of electrolytes is one of the determinant factors for the good energy storage performance of AZIBs and the potentials of the side reactions involving hydrogen evolution reactions and oxygen evolution reactions, are sensitive to the pH value and therefore are determined by the composition and concentration of the aqueous electrolyte. It is also known that a large number of byproducts at the cathode after continuous charging and discharging will be produced and those byproducts are mainly composed of zinc salts, which are responsible for the increase of interfacial impedance and capacity fading of cathodes during cycling. We herein focus on the parasitic side reactions and derived byproducts on cathode electrodes in the specific electrolyte solution.<sup>[9,10,55]</sup>

For cathode materials that enable  $\text{H}^+$  intercalation, the main parasitic byproducts are layered double hydroxides (LDHs) because the  $\text{H}^+$  consumption increases the local concentration of  $\text{OH}^-$  on the cathode side, as shown in Figure 2f. The generated

$\text{OH}^-$  will initiate the reaction with  $\text{Zn}^{2+}$  and anions, and the species of byproduct depend on the anion to some extent. For example, in  $\text{ZnSO}_4$  aqueous electrolyte,  $\text{Zn}_4\text{SO}_4(\text{OH})_6 \cdot 5\text{H}_2\text{O}$  will be the main byproduct, while  $\text{Zn}_5(\text{OH})_8\text{Cl}_2 \cdot \text{H}_2\text{O}$  byproduct can be easily detected if  $\text{ZnCl}_2$  aqueous electrolyte is used. Other byproducts, such as  $\text{Zn}_x(\text{CF}_3\text{SO}_3)_y(\text{OH})_{2x-y} \cdot n\text{H}_2\text{O}$  /  $\text{Zn}_{12}(\text{CF}_3\text{SO}_3)_9(\text{OH})_{15} \cdot x\text{H}_2\text{O}$  and  $\text{Zn}_4\text{ClO}_4(\text{OH})_7$  can be produced in  $\text{Zn}(\text{CF}_3\text{SO}_3)_2$  and  $\text{ZnClO}_4$  aqueous electrolyte, respectively.<sup>[56]</sup> Importantly, the crystalline structure of anion-based byproducts varies with different interlayer distances. To be specific, the interlayer distances are  $\approx 10$ ,  $\approx 11$ , and  $\approx 13$  Å for  $\text{Zn}_6(\text{NO}_3)_2(\text{OH})_8 \cdot 2\text{H}_2\text{O}$ ,  $\text{Zn}_4\text{SO}_4(\text{OH})_6 \cdot 5\text{H}_2\text{O}$  and  $\text{Zn}_x(\text{CF}_3\text{SO}_3)_y(\text{OH})_{2x-y} \cdot n\text{H}_2\text{O}$ , respectively. Among them,  $\text{Zn}_x(\text{CF}_3\text{SO}_3)_y(\text{OH})_{2x-y} \cdot n\text{H}_2\text{O}$  with the largest interlayer exhibits the best capacity improvement because of the widened 3D  $\text{Zn}^{2+}$  diffusion channel.<sup>[57]</sup> Besides the primary factor of electrolyte pH, other factors, such as dissolved  $\text{O}_2$ ,  $\text{Mn}^{3+}$  ions, and free water, have also been reported to affect the formation of LDHs products.<sup>[58]</sup> The role of these substances is not yet fully understood. Several positive effects have been proposed, including the stabilization of the chemical environment of cathode materials (i.e., pH of electrolytes) and the prevention of cathode dissolution.<sup>[56a,d,59]</sup> On the other hand, negative impacts, such as an increase in interfacial impedance and the consumption of electrolyte and Zn sources have also been identified.<sup>[60]</sup> The advantage and disadvantage of LDHs are actually defined. For any cathode materials involving  $\text{H}^+$  intercalation, the increase of localized  $\text{OH}^-$  concentration is inevitable, and LDHs with large ionic resistance has to be produced to buffer the pH variation. Instead of solely attributing improved cycling stability to the formation of LDHs, it may be more appropriate to view this as a result of self-regulation within the electrolyte. It is necessary to recognize that this passive adjustment may not be the most optimal solution, as its effectiveness is limited. A verified and preferred solution for this dilemma is to introduce pH buffering additives such as  $\text{ZnO}$ ,  $\text{La}(\text{OH})_3$  and  $\text{Mg}(\text{OH})_2$  into the electrolytes, without causing bulk electrolyte consumption and impedance increase but sustaining a stable solution environment.<sup>[61]</sup>

In addition to LDH precipitates, other byproducts that mainly persist in vanadium cathodes. Previous work also demonstrated that severe voltage and capacity decay over cycling was observed in polyanionic  $\text{VOPO}_4 \cdot x\text{H}_2\text{O}$  (VOP), suggesting the instabilities of the  $\text{VOPO}_4 \cdot x\text{H}_2\text{O}$ . Two possible degradation pathways of VOP in aqueous electrolytes can be concluded: a) the decomposition of VOP into solid  $\text{VO}_x$  together with the formation of  $\text{PO}_4^{3-}$  into the electrolyte. b) the dissolution of VOP into oxovanadium ions and  $\text{PO}_4^{3-}$  ions.<sup>[48c]</sup> Similar to the byproducts as discussed above, their identifications should also be coupled with some advanced characterization techniques to better understand the electrochemical Zn storage process. For example, the irreversible formation of inactive  $\text{ZnO}$  byproduct in spinel  $\text{ZnMn}_2\text{O}_4$  cathode during charge/discharge has been characterized by in situ Raman and ex situ XRD investigation. The  $\text{ZnO}$  byproduct could cause capacity fading and limited cycling performance.<sup>[62]</sup>

The parasitic byproduct formation remains one of the most essential and elusive challenges in AZIBs, which inevitably leads to unsatisfactory cycling performance, especially in the most commonly focused Mn-based and V-based cathodes. This

problem is more severe when the AZIBs operate under a low current density and high temperature, which is not sustainable and practical for grid-scale applications.

### 2.2.3. Phase Change

The phase change is a structural distortion for inorganic cathodes with specific crystal structures and that primarily relies on intercalation/de-intercalation storage mechanisms. Due to the large size (0.76 Å) and strong electrostatic attraction,  $\text{Zn}^{2+}$  can easily and tightly bond with the electronegative atom (i.e., the oxygen atom), resulting in significant stress inside the host materials during insertion/extraction and leading to structural collapse, or phase transition, Figure 2g.<sup>[13,63]</sup> This problem is also found in chalcogenides-based and Mn-based cathodes with various polymorph species.<sup>[40]</sup> For example, irreversible phase transformations have been observed in  $\text{MnO}_2$  polymorphs including  $\beta$ -,  $\gamma$ -, and  $\delta$ -polymorphs after a prolonged cycling performance, resulting in the formation of spinel  $\text{ZnMn}_2\text{O}_4$  phase. The formation energy of  $-1293.3$  kJ mol<sup>-1</sup> for  $\text{ZnMn}_2\text{O}_4$  makes the compound very stable, and the Zn extraction during the charging is highly unfavorable. The spinel  $\text{ZnMn}_2\text{O}_4$  also has high Zn migration barriers that hinder the diffusion of  $\text{Zn}^{2+}$  ions into the  $\text{ZnMn}_2\text{O}_4$  lattice.

Though it is widely recognized that the cathode will undergo significant volume change during the insertion/extraction of  $\text{Zn}^{2+}$  or other charge carriers, there is still a lack of systematic investigation regarding the microstructural or macrostructural variation of cathode materials. These findings will be instructive in understanding the storage mechanism and degradation mechanism of the intercalation cathodes.

### 2.2.4. Low Theoretical Capacity

Similar to the redox potential, the theoretical capacity of a specific cathode material also depends on its chemical nature. Generally, the theoretical capacity of a material is positively correlated to the electron transfer number ( $n$ ) but negatively correlated to the molar mass ( $M_w$ ) of the material, Figure 3a. Mn-based and V-based cathodes have multi-valence states and relatively small molar mass, enabling multi-electron redox reactions and therefore possess excellent theoretical capacity.<sup>[11a,64]</sup> In contrast, materials with large structure skeletons deliver low capacity in AZIBs, such as PBAs, organic materials, and polyanionic cathodes. Chalcogenides and metallic oxide cathodes exhibit low theoretical capacity with low electron transfer numbers ( $n = 1$ ) as the redox potentials of multi-electron reactions exceed the electrochemical stable windows of aqueous electrolytes. Capacity is an important indicator to determine the energy density of the battery, and the upper limit of this indicator is the theoretical capacity. How to minimize the size of molecules and activate reversible multi-electron reactions is the key to high theoretical capacity, which requires continuous exploration and mining of new chemistries. Concurrently, researchers need to be aware of the balance of the output capacity and cycle stability.



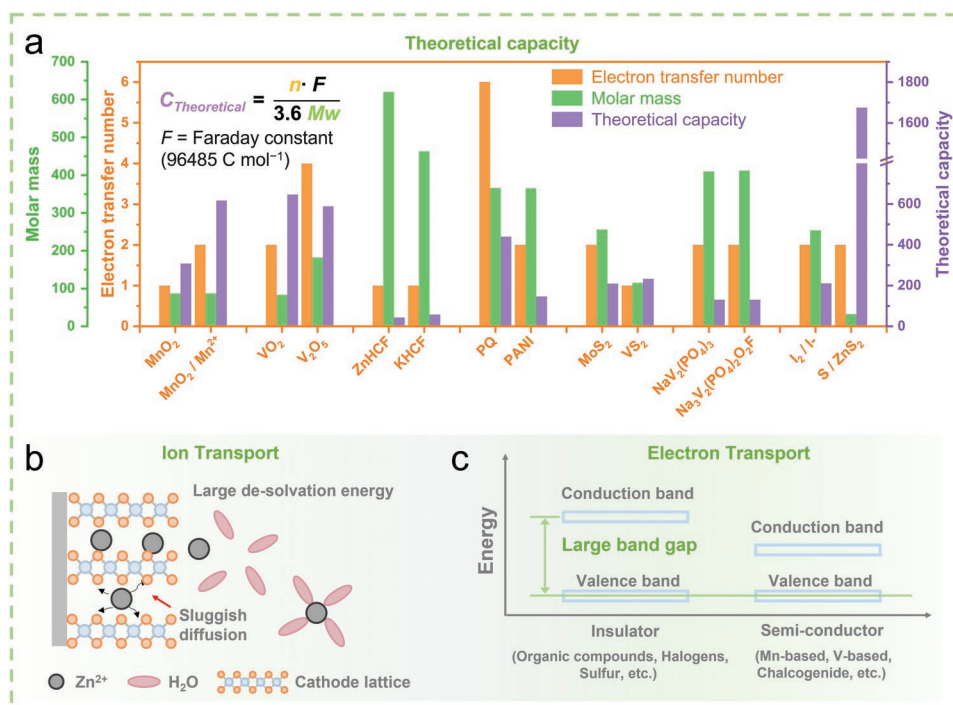


**Figure 3.** a) Comparison of electron transfer number, molar mass and theoretical capacity for AZIBs cathode material(s). Schematic for practical problems with challenging b) Ion and c) Electron transport.

### 2.2.5. Sluggish Charge Transfer Kinetics

The charge transfer kinetics of one electrode can be divided into two aspects, that is, ionic transport and electron transport kinetics. In terms of ionic transfer kinetics, compared with other monovalent charge carriers, such as  $\text{Li}^+$  or  $\text{Na}^+$ , the divalent  $\text{Zn}^{2+}$  presents intensive electrostatic interactions with  $\text{H}_2\text{O}$  molecules in aqueous electrolytes, which forms a solvent structure of  $\text{Zn}(\text{H}_2\text{O})_6^{2+}$ , accompanied by an increased molecule size of 5.5 Å (only 0.76 Å for  $\text{Zn}^{2+}$ ).<sup>[10a]</sup> Before the insertion of  $\text{Zn}^{2+}$  into cathode materials, a lot of energy is required to contribute to the desolvation procedure to release  $\text{Zn}^{2+}$  from the compact  $\text{H}_2\text{O}$  solvation sheath, Figure 3b. As a result, cathode materials involving  $\text{Zn}^{2+}$  intercalation reactions, such as Mn-based, V-based, and polyanionic cathodes, are hindered by desolvation penalty of hydrated  $\text{Zn}^{2+}$ . Additionally, the divalent  $\text{Zn}^{2+}$  induces strong electrostatic repulsion, leading to sluggish solid-state diffusion kinetics compared with that of the monovalent charge carriers.<sup>[65]</sup> The solid-state diffusion is also intimately related to the structure of cathode materials.<sup>[66]</sup> Take Mn-based cathode as example, the theoretical capacity is quite complex because of its crystallographic polymorphs that have entirely different ion diffusion channels. For example,  $\alpha\text{-MnO}_2$  with  $2 \times 2$  tunnels often delivers a capacity higher than  $250 \text{ mA h g}^{-1}$ , while the spinel  $\gamma\text{-MnO}_2$  merely presents a capacity lower than  $100 \text{ mA h g}^{-1}$ .<sup>[11a,67]</sup> Different from the intercalation/de-intercalation mechanism for aforementioned inorganic cathodes, organic cathodes that rely on ion-coordination reactions or halogen cathodes that employ conversion reactions are less dependent on the insertion of  $\text{Zn}^{2+}$ , resulting in favorable charge transfer kinetics.<sup>[31b,68]</sup>

The external electronic circuit of batteries is established on the stable connection between the cathode and anode. In AZIBs, the Zn anode is a good electronic conductor, while most cathode materials exhibit unsatisfactory electronic conductivity, Figure 3c. For example, Mn-based, V-based, and chalcogenide materials are semiconductors with inferior electron conductivity.<sup>[69]</sup> To maintain a good conductive network, a large number of conductive species (at least 20 wt.%) is needed, resulting in the “sacrifice” of active mass loading in the cathode electrode.

The electrochemical storage behavior of the cathode material largely depends on the kinetics of charge transfer, where the sluggish kinetics leads to the large electrochemical polarization, resulting in less-than-ideal storage capacity and inferior rate capability. Currently, the underlying mechanism of the solvation/de-solvation behaviors near the electrode/electrolyte interface is still unknown and understanding of key parameters controlling the diffusion of  $\text{Zn}^{2+}$  ions in different cathodes will be meaningful to tailoring cathode materials with boosted rate performance and high capacity.

### 2.2.6. Challenges for Practical Application

Fundamental research on cathode materials and the related energy storage mechanism made considerable contributions to the development of AZIBs by providing basic knowledge to both academia and industry. However, most of the research results from academia cannot directly transfer to practical devices for grid-scale application because of the lack of understanding of industrial requirements. In this case, we emphasize

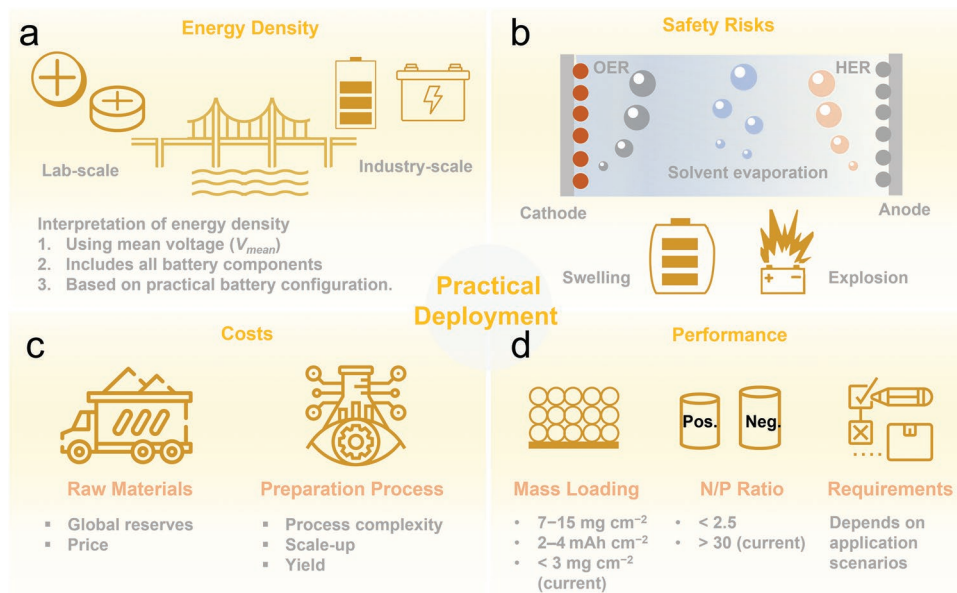


**Figure 4.** Obstacles to practical application of AZIBs. a) Energy density, b) Safety risks, c) Costs, and d) Performance.

the following key parameters that are widely focused on in energy storage systems and re-evaluate those parameters in AZIBs, in order to make the academic research toward the practical deployment in grid-scale energy storage.

**Energy Density:** In the case of batteries, specific energy density is intimately coupled to each other by the battery chemistry and choice of battery materials. Commercial batteries such as LIBs exhibit balanced performances in terms of energy density, power density, service life, safety, self-discharge performance, operating temperature range, and cost, in which energy density is the most important parameter being considered by both academia and industry. This is because the energy density can determine the maximum potential of a battery. The value of a battery is evaluated by the total usable energy (Wh) and the price of a battery is represented by the price of energy (US\$ kW<sup>-1</sup> h<sup>-1</sup>), regardless of battery size or mass.<sup>[70]</sup> Therefore, the low energy density of energy storage systems tends to occupy more cell volume and adds to its manufacturing and installation costs. However, different from the application of LIBs in electric vehicles with stringent design and performance requirements, an energy density over 50 Wh kg<sup>-1</sup> is sufficient for AZIBs in terms of stationary applications.<sup>[55,71]</sup> Another important factor is the exact interpretation of the obtained energy density in research, which should be verified in accordance with the accepted industry codes and standards, **Figure 4a**. Because the working voltage (V) gradually decreases with the depth of discharge, the mean voltage ( $V_{mean}$ ) should be used to calculate the electrical energy, instead of the open-circuit voltage ( $V_{ocv}$ ). Furthermore, the measured capacity decreases as the discharge current increase. In most cases, the cell capacity in AZIBs is limited by the cathode capacity, so the energy density is often estimated by simply multiplying the obtained capacity by the  $V_{ocv}$ , taking into consideration the Zn anode, but neglecting the mass of other components such as the electrolytes, separator, current collectors, and the packaging element.<sup>[72]</sup> Therefore, most of the energy densities are

somewhat overestimated. In addition, most of the reported energy densities calculated in scientific papers are based on a coin type, Swagelok, or a specific model cell, which are often far away from those of practical cells (cylindrical type, prismatic type, and pouch type).

**Safety:** Cost alone does not guarantee success. Mass-scale deployment of AZIBs also requires major improvements in performance, reliability, materials availability and stability.<sup>[73]</sup> Another important performance parameter for AZIBs should be safety, this is because, with grid-scale systems, the impact of a single incident can have substantially larger consequences than with smaller units. This shows that safety is indispensable for gaining the confidence of the user, investor, and insurer and holds precedence over its widespread adoption. Though aqueous systems are widely recognized as a safer alternative than classical LIBs with an organic electrolyte, aqueous batteries are not necessarily inherently safe due to rapidly increasing internal pressure caused by side reactions of gaseous products or uncontrolled high-temperature thermovaporization, **Figure 4b**. For cathode materials, the challenges associated with the formation of gas evolution and thermal phase changes can ultimately cause mechanical deformation of the cell components, leading to safety issues in the cell. It is therefore necessary to determine whether the selected cathode material is intrinsically safe and reliable or whether potential safety hazards can be solved by solutions before the start of the practical deployment.

**Cost Competitiveness:** The academia emphasizes impressive electrochemical performance, whereas the battery cost and preparation technique are mostly disregarded. However, for AZIBs to be successfully deployed, the cost and performance characteristics are important and will need to be cost-competitive with conventional technologies. An independent study suggested a target cost for grid-scale energy storage at < US\$100 per kW h (and power at < US\$600 per kW).<sup>[74]</sup> Since cathode materials largely determine the cost of AZIBs, the electrodes should be

preferably chosen from abundant and cost-effective materials, Figure 4c. Preparation process issues are also a huge obstacle to industrial application. For instance, the hydrothermal method and the modified co-precipitation method are major synthetic routes for cathode material production.<sup>[75]</sup> Considering these synthetic approaches involve complex mixing, drying, and high-temperature sintering processes, the cathode material production cost is still too high.<sup>[76]</sup> It should be noted that some newly developed methods are claimed to be cost-effective for synthesizing cathode materials in both laboratory-scale and pilot-scale tests, while there is no quantitative assessment of the potential to reduce the cost. Processes involving hazardous chemicals or expensive equipment, and low yield of materials cannot be neglected as well.

**Performance:** In terms of practical application, the following two parameters are critical for cathode materials in terms of performance evaluation, Figure 4d. a) Mass loading. The electrochemical behavior at high mass loading of cathode materials determines the electrochemical properties of AZIBs. Although electrochemical performance can be evaluated in thin electrodes with low active material loading (<3 mg cm<sup>-2</sup>), electrochemical performances simply do not scale with high mass loading. If active materials have low electronic conductivities, a large number of conductive species will be required to build up a conductive network. Especially, when a high mass loading is required for practical deployment (7 to 15 mg cm<sup>-2</sup>), the challenge of inadequate electronic conductivity will be magnified due to the lack of integrated conductive networks.<sup>[77]</sup> The introduction of abundant non-active material components (conductive species and binders) will eventually decrease the active material mass ratio, which results in inferior energy density. The mass loading should be high enough that an areal capacity of 2 to 4 mA h cm<sup>-2</sup> is reached. b) Negative/positive ratio (N/P ratio). For LIBs, the N/P ratio is generally set to 1.05 to 1.15 to avoid the deposition of Li on the graphite anode during charge, and this value can be further increased to 2.5 if a Li metal anode applies. However, performance reported in the literature has often been obtained under a higher N/P ratio for AZIBs (usually > 30:1), while they are only of limited value for industrial production.<sup>[78]</sup>

Different applications have different performance requirements, for example, such as loading shifting, the systems are required to MWh or even GWh levels that are capable of discharge duration of up to a few hours or more.<sup>[71]</sup> This kind of application requires high round-trip efficiency and long deep-cycle life, along with low operation and maintenance costs. However, for frequency regulation, the capacity may not need to be long-lasting but must have a long cycle life. How to develop the cathode materials to assemble AZIBs to fulfil various application scenarios is still a big challenge.

### 3. Strategies for Developing Advanced Cathodes

Notwithstanding excellent electrochemical performance can be obtained, the cathode materials still face respective shortcomings. To mitigate corresponding issues for these cathode materials, plenty of studies have been carried out on introducing novel structural designs and compositions. This section revisits

the current efforts in material engineering, electrolyte regulations, separator modifications, etc., aiming to reveal the underlying design principles and inspire innovative strategies for future studies.

#### 3.1. Achieving High Redox Potential

The elegant introduction of extra redox centers with low Fermi level into targeted materials has become a prevalent strategy to boost electrochemical activity and conductivity, which has been extended to the modification of cathode materials in AZIBs, Figure 5a. It is believed that Mn and V are important active elements in most cathode materials and incorporating V or Mn elements into cathode materials without V and Mn elements would be a practical tactic. For instance, Wu et al. reported that when Mn is incorporated into the polyanionic cathode of Na<sub>3</sub>V<sub>2</sub>(PO<sub>4</sub>)<sub>3</sub>, a significant increase in both capacity and working voltage (89.1% capacity retention after 3000 cycles at 5.0 A g<sup>-1</sup>) can be observed in the Na<sub>4</sub>VMn(PO<sub>4</sub>)<sub>3</sub> due to a two-step electron transfer mechanism between V<sup>3+</sup>/V<sup>4+</sup> and Mn<sup>3+</sup>/Mn<sup>2+</sup> redox couple.<sup>[79]</sup> Similarly, by introducing the Co<sup>2+</sup>/Co<sup>3+</sup> redox couple into the CoFe(CN)<sub>6</sub> PBAs, the two-species redox reaction of Co<sup>2+</sup>/Co<sup>3+</sup> and Fe<sup>2+</sup>/Fe<sup>3+</sup> contributes CoFe(CN)<sub>6</sub> PBAs a high discharge voltage of 1.75 V with a high capacity of 173.4 mA h g<sup>-1</sup>, which is much higher than that of the PBAs with single Fe<sup>2+</sup>/Fe<sup>3+</sup> couple (≈60 mA h g<sup>-1</sup> at an operating voltage of 1.2 V).<sup>[17a]</sup> However, the introduction of new redox sites may possibly increase the molecular mass, resulting in a decreased capacity (will be discussed in the following). Besides, its applicability would be a huge challenge since not all the redox couples can be mixed together due to intrinsic incompatibility or synthesis issues.

Taking advantage of oxygen redox (O<sup>2-</sup>/O<sup>-</sup>) is another facile and efficient strategy in layered oxide cathodes to improve the potential and increase the capacity.<sup>[80]</sup> For instance, Wan et al. discovered that the activation of the oxygen redox process not only led to increased capacity and a higher V<sub>ave</sub> of the Zn/VOPO<sub>4</sub> batteries, but also improved rate and cycling performance.<sup>[30]</sup> This is because of the increase in the electron density of the oxygen atoms due to the existence of P-O covalence, which weakens the V-O covalence compared with that of the V<sub>x</sub>O<sub>y</sub> polyhedra. Therefore, the oxygen redox reaction was activated at 1.82/2.02 V for the VOPO<sub>4</sub> cathode and ≈27% additional capacity can be provided after the activation of oxygen redox reactions. Notably, the occurrence of anionic redox reactions depends on the design of new cathode materials and the appropriate selection of electrolyte formulas. The reversibility of the anion redox is another issue as the irreversible release of O<sub>2</sub> inevitable leads to capacity degradation and batteries safety.

According to the Nernst equation, the redox potential of cathodes can be altered when the species or the concentrations of redox substances are changed, which can be easily realized by the strategy of electrolyte engineering, Figure 5b. For instance, the traditional Mn<sup>3+</sup>/Mn<sup>4+</sup> redox pair in the mild-acid electrolyte can offer a redox potential of 1.3 V based on the intercalation mechanism while activating the Mn<sup>2+</sup>/Mn<sup>4+</sup> redox pair can increase the redox potential from 1.3 to 1.9 V based on the conversion mechanism. The Mn<sup>2+</sup>/Mn<sup>4+</sup> redox pair can be

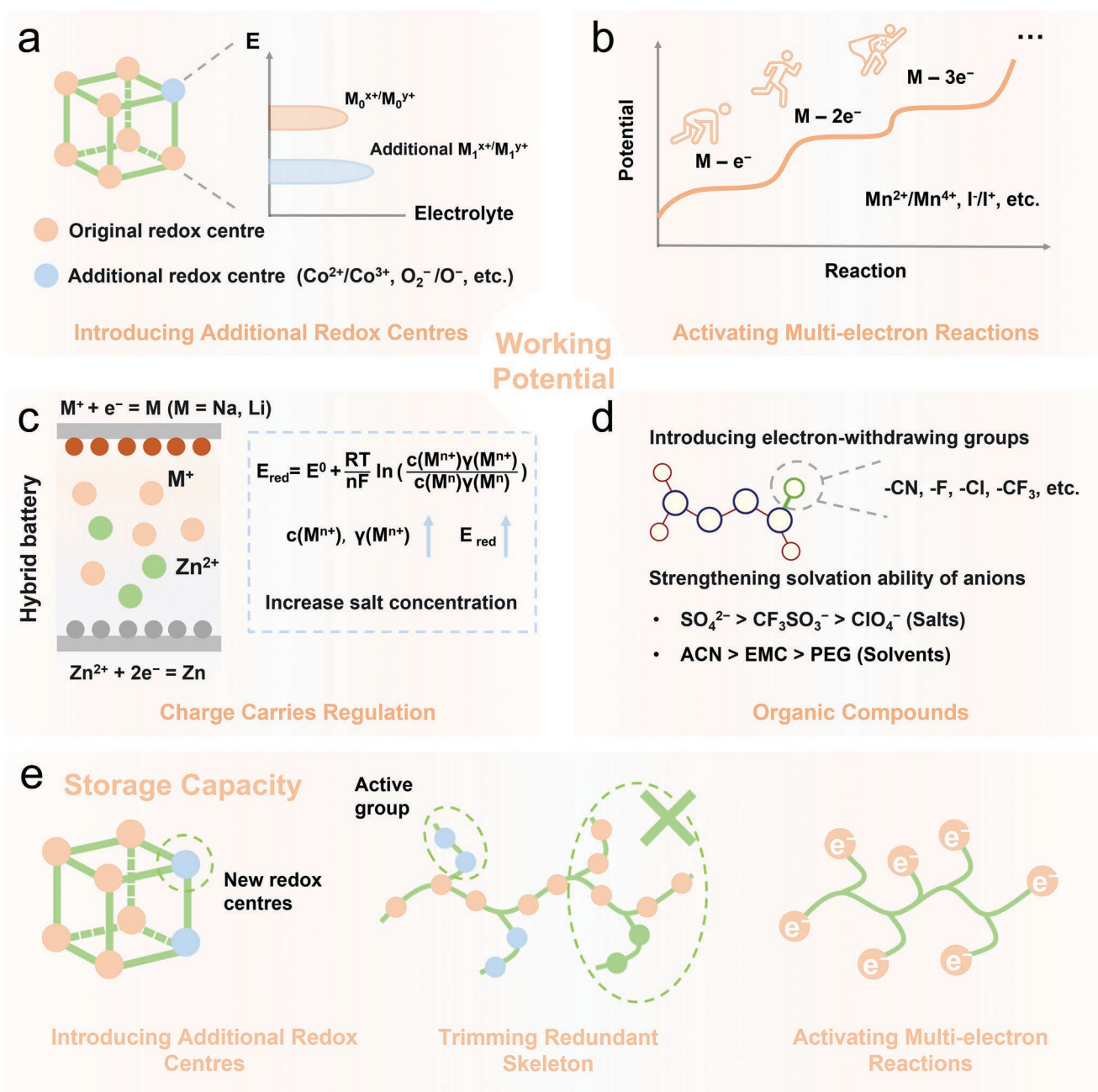


**Figure 5.** Development of high working potential of cathode materials. a) Introduction of additional redox centers, b) Activation of multi-electron reactions, c) Regulation of charge carriers, and d) Strategies for organic compounds. e) Increasing storage capacity of cathodes.

dramatically enhanced by increasing the acidity of electrolytes to promote the dissolution of  $\text{Mn}^{2+}$  ions in the electrolyte.<sup>[81]</sup> Engineering the electrolyte from the mild-acid solution to an acetate-based near-neutral electrolyte can also unlock the  $\text{Mn}^{2+}/\text{Mn}^{4+}$  redox chemistry because the acetate ion could lower the dissolution barrier of  $\text{MnO}_2$ .<sup>[81c]</sup> Besides, the  $\text{I}^0/\text{I}^+$  redox couple can be activated by introducing the  $\text{Cl}^-$  additive into the electrolyte due to the  $\text{I}^+$  dissolution can be efficiently controlled by the formation of the  $\text{ICl}$  intermediate. In this case, the redox potential can be further increased from 1.28 to 1.65 V in  $\text{Zn}/\text{I}_2$  batteries. Other electrolyte additives containing exotic cations

(i.e.,  $\text{Li}^+$  or  $\text{Na}^+$ ) can establish hybrid ion batteries by concurrently using the exotic cation and  $\text{Zn}^{2+}$  ions as charge carriers to increase the redox potential of the battery further.<sup>[82]</sup> Introducing cathode materials (i.e.,  $\text{LiMn}_2\text{O}_4$ ) with good compatibility with exotic cations will be a prerequisite factor. Besides, according to the Nernst equation, increasing the zinc salt concentrations of the electrolyte can increase the redox voltage to higher values because the activity of  $\text{Zn}^{2+}$  ions in the electrolyte is enlarged, Figure 5c.<sup>[83]</sup> For example, when the concentration of  $\text{ZnCl}_2$  electrolyte was increased from 1 to 30 M, the redox voltage of the  $\text{Zn}/\text{Ca}_{0.2}\text{V}_2\text{O}_5 \cdot 0.8\text{H}_2\text{O}$  was increased by

0.15 V.<sup>[59a]</sup> While the potential of Zn/Zn<sup>2+</sup> also increases with the salt concentration, which may offset the augmentation of cathode potential. The success of this strategy greatly depends on the species and activity of the charge carriers, which still requires deep understanding. Even if the increase in electrolyte concentration should change the redox potential, the ionic conductivity and the energy density are decreased, along with the increase in production cost.

Due to the unique charge storage mechanism of organic materials, strategies to improve the redox potential are different from inorganic cathodes, Figure 5d. Taking *p*-type organic cathodes as an example, the cathode potential originates from two-step reactions. The first step is the oxidation of *p*-type organics removes electrons from the *p*-conjugated structure and the second step is that anions balance the positive charge left on the organics from the electrolyte. Therefore, previous research attempted to increase the redox potential by either improving the high electron affinity of targeted organics by introducing electron-withdrawing groups (-CN, -F, -Cl, and -CF<sub>3</sub>) or choosing appropriate electrolytes to enable compact anion solvation structure formation during cycling.<sup>[84]</sup> Adjusting substituent positions and averaging the electron cloud density via aromatic  $\pi$  structures are also beneficial for the first step.<sup>[85]</sup> The electrolyte engineering can be realized by choosing suitable salts (SO<sub>4</sub><sup>2-</sup> > CF<sub>3</sub>SO<sub>3</sub><sup>-</sup> > ClO<sub>4</sub><sup>-</sup>) or solvents (acetonitrile > ethyl methyl carbonate > polyethylene glycol) during the electrolyte preparation.<sup>[86]</sup> It should be noticed that the cycle stability may be compromised because the strengthened binding energy also leads to slow electrode kinetics and heterogeneous reactions. It is recommended that additional efforts be made to expand our knowledge regarding the correlation between the charge storage behaviors of organic cathodes and the constituents of the electrolyte.

### 3.2. Increase the Storage Capacity

The number of transferred electrons and molecular mass dictates the theoretical capacity of a cathode material. Increasing the number of transferred electrons and decreasing the molecular mass of cathode materials will be the most intriguing strategies to improve the storage capacity, Figure 5e.

#### 3.2.1. Redox Centers Engineering

The incorporation of new redox centers can improve the number of transferred electrons to enhance the storage capacity, but at the cost of a marginal increase in the molecular mass. Taking conventional Na<sub>3</sub>V<sub>2</sub>(PO<sub>4</sub>)<sub>3</sub> cathode (M<sub>w</sub>: 455.7 g mol<sup>-1</sup>) as an example, it can only deliver a capacity of 106.5 mA h g<sup>-1</sup>, while the Na<sub>4</sub>V<sub>Mn</sub>(PO<sub>4</sub>)<sub>3</sub> (M<sub>w</sub>: 482.7 g mol<sup>-1</sup>) with the introduction of Mn<sup>2+</sup>/Mn<sup>3+</sup> redox couple gives the capacity of 230.7 mA h g<sup>-1</sup>.<sup>[79]</sup> This strategy is particularly suitable for cathode materials with inherently large molecular mass since the introduction of additional redox pairs will not significantly increase the molecular mass. Additionally, for organic cathodes with large molecular mass, removing inactive skeletons from the molecular structure without affecting the structural stability will be an alternative way to improve the capacity of the organics.<sup>[87]</sup> Introducing

atomic defects such as anion (oxygen, sulfur, selenium, *etc.*) and cation (manganese, vanadium, *etc.*) vacancies may become another advisable choice to boost the capacity but not contribute to the molecular mass. The introduction of defects in cathodes has been claimed to enhance the electrochemical performance of AZIBs by improving the Zn<sup>2+</sup> transfer kinetics and electrochemical reactivity (will be discussed later), but the quantities and sites of defects have never been discussed, which should be emphasized and need further exploration.

#### 3.2.2. Activating Multi-Electron Redox Reactions

Single redox with low capacity or low working potential dominates especially for inorganic materials, such as Mn<sup>3+</sup>/Mn<sup>4+</sup>, V<sup>4+</sup>/V<sup>5+</sup>, and I<sup>0</sup>/I<sup>-</sup>, *etc.* Activating two-electron redox pairs may be an intriguing solution, especially for cathode materials with multi-valent elements. It is found that activating V<sup>3+</sup>/V<sup>5+</sup> two-electron reactions in LiV<sub>3</sub>O<sub>8</sub> cathode under high cut-off voltage of 1.6 V can obtain an appreciable capacity of 557.5 mA h g<sup>-1</sup>, although a large polarization happens at high current densities.<sup>[88]</sup> For Zn//I<sub>2</sub> batteries, with the support of F<sup>-</sup> and Cl<sup>-</sup> additives, the resultant multi-valent conversion of I<sup>-</sup>/I<sup>0</sup>/I<sup>+</sup> led to a significantly improved capacity of 207 mA h g<sup>-1</sup>, benefiting from two well-defined discharge plateaus at 1.65 and 1.3 V. The high voltage plateau region at 1.6 V contributed to over 52% capacity and 69.8% energy output.<sup>[33]</sup> In addition, Multi-electron redox pairs can also be achieved in organic cathodes if increasing the number of active functional groups (*i.e.*, carbonyl groups).<sup>[46]</sup> Clearly, the energy density of iodine-based cathodes can be further improved by elevating the working potentials, but at the cost of forming of polyiodide and irreversible capacity loss. Notably, the operation of two-electron redox pairs requires high working potential, which needs aqueous electrolytes with superior oxidative stability. Therefore, further explorations from the perspective of cathode materials, electrolytes, and their interfaces are needed.

### 3.3. Accelerate Reaction Kinetics

One of the origins of the capacity fading of the cathode in AZIBs is that the successfully intercalated Zn<sup>2+</sup> ion cannot be fully de-intercalated out of the interlayer and then stuck in the interlayer, limiting the Zn<sup>2+</sup> diffusion.<sup>[89]</sup> Eventually, the storage site of the host will be permanently occupied and induce capacity loss. Therefore, strategies capable of promoting Zn<sup>2+</sup> diffusion are required to address this problem. Given that electrochemical reactive kinetics closely depends on the structure, surface chemistry, morphology, *etc.*, varied approaches have been employed to optimize the cathode materials for improved ionic/electronic conductivity. This section summarizes different modification strategies and analyses the corresponding working mechanisms.

#### 3.3.1. Pre-Intercalation Effect

Large interlayer spacing is required for layered cathode materials to provide migration channels for sufficient Zn<sup>2+</sup> ions

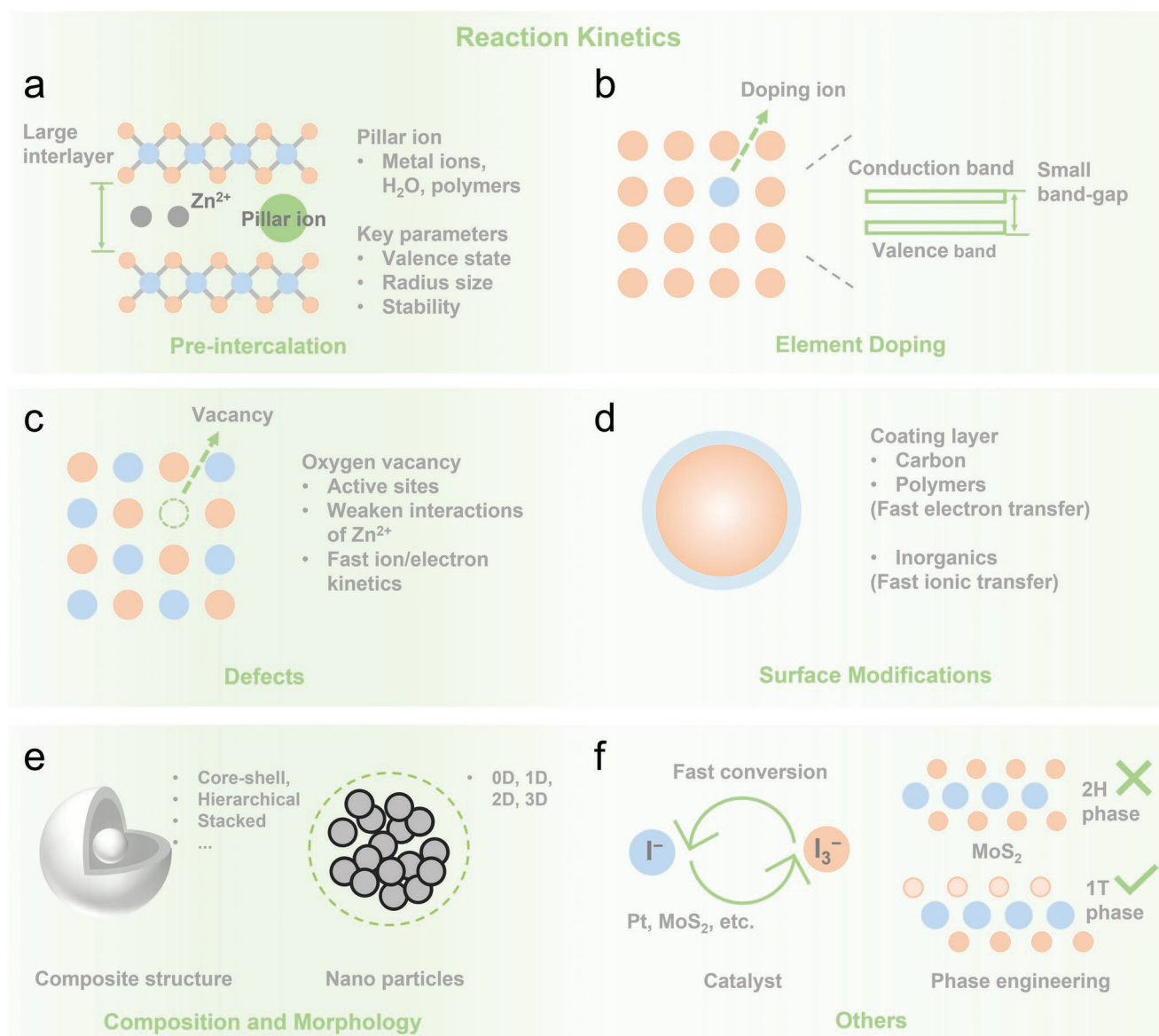


**Figure 6.** Increasing reaction kinetics of cathode materials. a) Pre-intercalation, b) Element doping, c) Defects, d) Surface modification(s), e) Composition and morphology engineering, and f) Other.

flux during cycling.<sup>[63,75]</sup> Nevertheless, most reported cathodes fail to provide wide-open channels. Among the popular strategies, recruiting exotic ions or molecules as pillars to enlarge the interlayer distance of the host is representative, **Figure 6a**. Specifically, a range of metal ions including Fe<sup>2+</sup>, Mg<sup>2+</sup>, Ni<sup>2+</sup>, Mn<sup>2+</sup>, Li<sup>+</sup>, Na<sup>+</sup>, K<sup>+</sup>, and even NH<sub>4</sub><sup>+</sup> has been selected into efficient hosts with large interlayer spacing and robust structures (*i.e.*, layered vanadium oxides).<sup>[90]</sup> The accessibility of the pre-intercalation strategy closely depends on if the selected exotic ions are well-matched with the ionic radius of the host, instead of the valence state.<sup>[91]</sup> For example, Ag<sup>+</sup> with a large radius size cannot be inserted into the V<sub>x</sub>O<sub>y</sub> cathode. The pre-intercalation contributes to the long-term cycle stability by stabilizing the host because of the formation of covalent linkage with host frameworks. However, it is still unknown if the exotic

ions can be extracted from the host structure during cycling. This is strongly related to the electrostatic attraction between the exotic ions and the host framework. Normally, monovalent ions have a weaker binding energy with the lattice oxygen than that of Zn<sup>2+</sup> ions and the multi-valent ions.<sup>[65]</sup> The presence of a large number of exotic ions offers a flexible nature to the host framework structure but would induce unstable structure and structural degradation if they are extracted from the host materials. Therefore, host materials, exotic ions, and related binding energy should be carefully considered to keep the structural stability with enlarged interlayer spacing. The quantity and distribution of exotic ions inserted into the host materials cannot be neglected as well. Besides, it is believed that zero-valent metal species can be successfully intercalated into layered materials without altering the valence state of the host elements and

damaging the structural robustness of the host materials, while the direct intercalation of zero-valent metals in bulk, layered materials has rarely been achieved in AZIBs.<sup>[92]</sup>

Similar situations have been extended to other exotic molecules including H<sub>2</sub>O, small molecules, and polymers. The insertion of Zn<sup>2+</sup> hydrate can not only expand the interlayer spacing of the host material but also mitigate the strong charge interactions between Zn<sup>2+</sup> ions and the host framework by providing a functional charge shield to favor the intercalation/deintercalation of Zn<sup>2+</sup> ions.<sup>[10a]</sup> In addition, conductive polymers including poly(3,4-ethylenedioxythiophene) (PEDOT) and polyaniline can expand the interlayer spacing of host materials.<sup>[93]</sup>

It should be noted that the pre-intercalation strategy may only be dedicated to the layered oxides cathodes, while other kinds of layered materials such as metal chalcogenides, MXene, and even carbon materials are encouraged to be explored. In addition, the synthetic procedures should be further optimized to quantitatively control the introduced exotic ions, engineer the intercalated sites, and influences on the morphology and local crystal microenvironment. The electrolyte formulas are also suggested to be regulated to maintain the pillared structure, therefore improving the reversible capacity, accelerated kinetics, and cycling performance. *In situ/operando* characterizations are also encouraged to understand the pre-intercalation process and results, in order to establish correlations among the synthesis, structural change, and electrochemical properties.

### 3.3.2. Element Doping

Different from the pre-intercalation that is exclusive to layered materials, element doping is widely applicable to most inorganic cathodes in AZIBs. Doping cathode materials with metal or non-metal ions can tune the intrinsic electron structure to boost the electrode kinetics, Figure 6b. Long et al. reported that by increasing the doping concentration of Ni<sup>2+</sup> into Ni<sub>x</sub>Mn<sub>3-x</sub>O<sub>4</sub>, the Ni<sub>x</sub>Mn<sub>3-x</sub>O<sub>4</sub> (x = 1) cathodes can dramatically decrease the bandgap and improve the electronic conductivity in the Ni<sub>x</sub>Mn<sub>3-x</sub>O<sub>4</sub> crystal structures.<sup>[94]</sup> Zhang et al. also reported that the formation of N-doped MnO<sub>2-x</sub> branch with rich oxygen vacancies on conductive TiC/C nanorods can increase the electron densities and lower the bandgap of MnO<sub>2</sub>, thus enhancing the activity of MnO<sub>2</sub> for AZIBs.<sup>[95]</sup> However, how to realize the precise control of atom occupancy is also a great challenge. The effect of the occupied position on tuning the reaction dynamics and the doping content on the structural stability of cathode materials is still unknown. Although both metal and non-metal heteroatom doping modification is expected to improve the transfer kinetics, comprehensive understandings are required to provide guidance in material engineering and design. Theoretical and computational understandings are powerful in understanding the structural change in material science, which could help to evidence ideas and explore possible reasons for performance enhancement.

### 3.3.3. Introducing Defects

Incorporating defects is beneficial to capacity and charge transfer kinetics because defects can provide additional sites

and manipulate the electronic and crystal structures.<sup>[40,65,96]</sup> In material science, the defect of a material always refers to the vacancy, which can be mainly divided into anion and cation vacancy. Considering manganese oxides and vanadium oxides are dominant cathode materials and the low formation energy, the oxygen vacancy (O<sub>vac</sub>) is the most studied anion vacancy, Figure 6c. Basically, the effects of the introduction of O<sub>vac</sub> can be summarized as 1) providing more active sites to improve the capacity; 2) weakening the electrostatic intercalation of Zn<sup>2+</sup> ions with the host materials; 3) boosting the ion/electron transport kinetics.<sup>[97]</sup> However, there are still many open questions to be answered. For example, considering the current progress is mainly focused on the study of the single defect, if the introduction of multiple defects can induce synergistic effects is still unknown. Controlling the defect sites and concentration is still challenging and requires advanced synthesis protocols and suitable precursors. Importantly, if the defects can keep the crystal structure stable is not determined, especially during the cycling. Meanwhile, the previously reported S, Se, and Te vacancies in materials for alkaline ion batteries would also be promising and can be trailed in cathodes for AZIBs.<sup>[98]</sup>

### 3.3.4. Surface Engineering

Surface coating is a versatile strategy to address the problems such as inferior transfer kinetics, structural degradation, and cathode dissolution (will be discussed in the following). Both inorganic phase and organic species can be served as coating materials, Figure 6d. For the organic coating approach, conductive carbon (*i.e.*, carbon nanotube, graphene, and porous carbons) and polymer coating (*i.e.*, PEDOT) were used to improve the electronic conductivity of pristine cathode materials, such as MnO<sub>2</sub>, V<sub>2</sub>O<sub>5</sub>, Mn<sub>3</sub>O<sub>4</sub>, *etc.*<sup>[65]</sup> The PEDOT coating layer can also improve the capacity by providing reversible adsorption/desorption sites.<sup>[99]</sup> Besides the organic coating, inorganic oxide coating is another promising strategy to improve the transfer kinetics by accelerating the transfer of ions through interfaces.<sup>[65,100]</sup> For example, by introducing the PO<sub>3</sub><sup>-</sup> groups on the surface of Co<sub>3</sub>O<sub>4</sub> ultrathin nanosheets, enhanced electrochemical performance can be achieved due to the weak attraction of electrons in the 3d orbital of Co ions, which lowers the energy barrier of the redox reaction of Co<sup>3+</sup>/Co<sup>4+</sup>.<sup>[101]</sup> A multiple surface engineering strategy was also reported by Liu et al. to fabricate the P-MnO<sub>3-x</sub>@Al<sub>2</sub>O<sub>3</sub> cathode material with oxygen vacancies, where Al<sub>2</sub>O<sub>3</sub> coating can stable the interface between the cathode and the electrolyte as well as boost the transfer kinetics, oxygen vacancies can enhance the electronic conductivity.<sup>[24a]</sup> Coating with inorganic species is also expected to be obtained via *in situ* preparation techniques during battery operation, which can minimize manufacturing steps and costs in practical production.<sup>[102]</sup> This coating layer would be similar to the formation of the solid-electrolyte interface that is widely reported in LIBs during the initial operation of batteries. However, the formation of cathode-electrolyte interface in aqueous electrolytes is debated and ambiguous because both cathode materials and the chosen electrolyte chemistry play key roles in determining the formation of this layer. The effect of coating can be quite profound, however, the relationship between the

electrolyte and the coating layer in transfer kinetics, reaction mechanism, and the change of physiochemical properties of the coating layer need to be further studied.

### 3.3.5. Engineering Cathode with Different Compositions and Morphology

The construction of composite cathodes can endow the composite material with new features and synergistically combine the advantages of a single material, Figure 6e. As a result, the composite cathode materials are expected to provide balanced and superior electrochemical performance.<sup>[103]</sup> Different from the coating strategy to form an intimate layer on the surface of active material, the formation of composite cathodes exhibits various modes including hierarchical structure, core-shell structure, stacked structure, *etc.*<sup>[104]</sup> The most widely studied compositing uses carbon as a complementary component. In addition to the multi-functions by the carbon coating layer, the carbon-based composite materials can alleviate the volume change of active materials during cycling. The formation of composite materials is widely reported in various cathode materials. Nevertheless, considering the existence of non-active carbon with large surface areas that would possibly take up a certain of space, the total volumetric energy density would be decreased. Besides, the employed carbon materials are usually graphene and carbon nanowires, which are much more expensive than common carbon species and bring the problem of high cost in terms of practical production. Exploring the relationship between the carbon content in composite materials and diffusion kinetics will benefit the development of composite materials in terms of high-energy-density and high-rate performance.

In addition, the morphology of the cathode material has a significant influence on the ionic/electronic transfer behavior, which is governed by a local combination of Ohm's law and Fick's law, and the transport rate can be estimated by the characteristic diffusion time ( $\tau^*$ ) according to an equation ( $\tau^* = L^2/\alpha D$ ), where  $D$  is the effective diffusion coefficient,  $L$  is the radius or half-thickness,  $\alpha$  is a geometric factor.<sup>[105]</sup> Based on this equation, the cathode with nanostructure has a smaller particle radius ( $L$ ) compared with that of the cathode with microstructure, providing a short transport path.<sup>[106]</sup> Generally, nanomaterials can be divided into four categories including 0D (nanodots and nanospheres), 1D (nanorods, nanowires, and nanotubes), 2D (nanosheets and nanofilms), and 3D (hierarchy) materials.<sup>[107]</sup> Among them, both 1D and 2D have the advantages of boosting transfer kinetics. However, the limitation of 1D transport dimensions and the self-stacking issue of 2D materials during cycling would inevitably weaken the reaction kinetics, especially for the thick electrode with high mass loading.<sup>[63,65,108]</sup> In this case, developing hierarchical 3D nanostructures with robust structures and accessible ionic transfer channels is desirable. Nevertheless, most cathode materials suffer from dissolution problems in aqueous electrolytes and the increase in the surface area of nanomaterials will undoubtedly worsen this problem. In addition, most of the 3D nanomaterials require complex synthetic procedures, which blocks the commercialization of

nanosized cathodes in AZIBs. Most importantly, the intrinsic low tap density owing to the loose stacking will result in low volumetric energy density, while the large surface area may exacerbate side reactions and lower the CE.<sup>[109]</sup> In this case, nano engineering is not as suitable as other modification strategies for battery materials.

In short, the design principles of advanced cathode materials with efficient transport kinetics should consider both composition and microstructure. From the perspective of microstructural design, a hierarchical cathode consisting of nanostructures that are encapsulated by conductive species to assemble into secondary microstructures will be promising. Porous structures with a suitable surface area can provide abundant transfer channels, which are also required for the microstructure. However, the dissolution issue of active materials in the hierarchical structure brings uncertainties and difficulties in maintaining the structural advantage. The extensive use of templates or precursors would also lead to a high production cost. In this case, it is therefore required to develop multiple strategies involving material science, electrolyte engineering, separator modification, and cell configuration regulation to achieve balanced performance.

### 3.3.6. Other Strategies

For iodine-based cathodes, the inferior electrode kinetics is related to the sluggish  $I^-/I_3^-$  redox pair, which can be improved by employing functional catalysts, such as Pt,  $MoS_2$ , and  $CoS$ , in order to lower the energy barrier and accelerate the charge transfer kinetics, Figure 6f.<sup>[110]</sup> MOF and PBAs have also been reported as catalysts to promote the conversion reaction by virtue of the unique Lewis-acidic metal centers.<sup>[111]</sup> Nevertheless, the cycling performance of the  $Zn//I_2$  batteries after adding functional catalysts is still unsatisfactory, which can be attributed to the degradation or the poisoning of the catalyst during  $Zn^{2+}$  ions intercalation/de-intercalation.<sup>[112]</sup> The utilization of a noble metal-based or MOF catalyst will greatly increase the cost of the cathode, which is not desirable for AZIBs that are targeted for grid-scale energy storage. Thus, developing catalysts with cost-effective feature, robust structures, and high catalytic efficiency is of great importance.

Besides the aforementioned strategies, some strategies are also used for particular cathode materials to improve the transfer kinetics, Figure 6f. For instance,  $MoS_2$  has different structural phases with different metal coordination geometries, including a trigonal phase (2H) or an octahedral phase (1T). Previous results indicate that  $MoS_2$  with high 1T phase content (70%) showed outstanding electrochemical performance due to the low  $Zn^{2+}$  ion diffusion energy barrier and metallic properties for good electronic conductivity.<sup>[113]</sup> It is demonstrated that the phase change strategy will be applicable to some inert cathode materials to promote the charge transfer kinetics.<sup>[114]</sup> Moreover, molecular engineering is beneficial to improving the intrinsic electronic conductivity of organic materials, such as expanding the  $\pi$ -aromatic conjugation structure, grafting active groups, and incorporating heteroatom doping, which have been verified as valid approaches.<sup>[85b,115]</sup>



### 3.4. Enhance the Cycle Stability

The electrochemical performance degradation of cathode materials is not only caused by poor ionic/electronic conductivity but also caused by the dissolution issue and poor structural/chemical stability, which is ubiquitous to all kinds of cathode materials. In this section, we mainly focus on practical strategies to tackle the issues of dissolution and structural/chemical stability in cathode materials.

#### 3.4.1. Electrolyte Engineering

Engineering the electrolyte has drawn much attention previously and this section will not comprehensively revisit its role in manipulating the electrochemical properties of anode and the anode-electrolyte interface but mainly focusing on stabilizing electrochemical and chemical stability of the cathode.<sup>[2,8b,116]</sup> Electrolyte engineering is not only beneficial to changing the redox potential but also conducive to suppressing the side reaction to regulate the parasitic byproducts, **Figure 7a**. Considering the dissolution of cations from cathode materials is a reversible reaction, the cation dissolution can be relieved by increasing the concentration of identical cations according to Le Chatelier's principle.<sup>[117]</sup> This concept has been successfully implemented in manganese-based cathodes to tackle the manganese

dissolution in AZIBs. The same result can also be found in other cathodes, such as  $\text{NaV}_3\text{O}_8$ , zinc hexacyanoferrate,  $\text{Co}_3\text{O}_4$ , etc.<sup>[38,118]</sup> Specifically, by adding appropriate amounts of  $\text{Mn}^{2+}$  into the electrolyte, the dissolution equilibrium of  $\text{Mn}^{2+}$  from the  $\text{MnO}_2$  cathodes can be regulated and suppressed. While a continuous increase in capacity at the initial discharge stage was observed in the electrolyte containing additional  $\text{Mn}^{2+}$  ions, which should be ascribed to the electro-deposition of excessive  $\text{Mn}^{2+}$  on the cathode. The ongoing deposition on the cathode will unavoidably consume the  $\text{Mn}^{2+}$  in the electrolyte and weaken the effectiveness of this kind of strategy.<sup>[119]</sup> Besides, the optimized amount of  $\text{Mn}^{2+}$  ions in lean electrolyte condition should also be investigated for practical applications.

Using high-concentration electrolytes (HCEs) is another effective strategy to mitigate the cathode dissolution owing to the scarce free water molecules with large saturability in the electrolyte solution.<sup>[87a,119c,120]</sup> This approach can be successfully implemented in inhibiting the cation dissolution in  $\text{V}_2\text{O}_5$ ,  $\text{MoO}_3$ , and  $\text{Zn}_3[\text{Fe}(\text{CN})_6]_2$  cathode materials when  $\text{ZnCl}_2$ -based HCEs employed. It is also reported that this strategy can be extended to dual-salt HCEs system, for instance, in 1.5 M  $\text{MgSO}_4$  + 0.5 M  $\text{ZnSO}_4$  or in 2.5 M  $\text{Mg}(\text{CF}_3\text{SO}_3)_2$  + 0.5 M  $\text{Zn}(\text{CF}_3\text{SO}_3)_2$  electrolyte, both of these two  $\text{Zn}/\gamma\text{Fe}_2\text{O}_3$  battery systems exhibit good rate performance. This is because the high  $\text{Mg}^{2+}$  concentration can suppress the formation of LDHs byproducts by forming  $\text{Mg}(\text{H}_2\text{O})_6^{2+}$  solvation shell.<sup>[121]</sup> Besides,

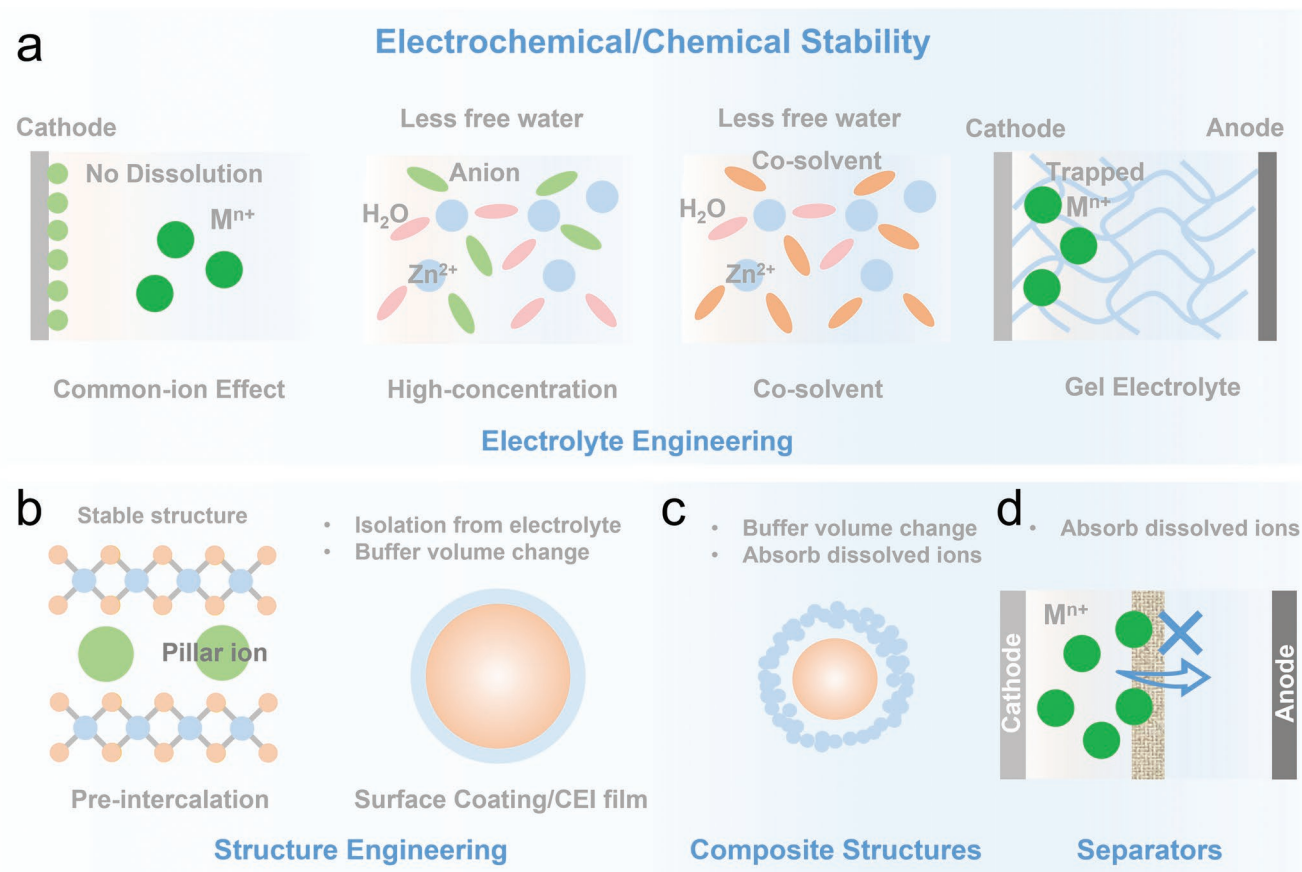


**Figure 7.** Boosting electrochemical/chemical stability. a) Electrolyte engineering, b) Structure engineering, c) Composite structures, and d) Separator design.

HCEs also avoid polyiodide formation by inhibiting the bonding between  $I_2$  and free  $I^-$  ion in electrolytes. Due to the high concentration of salts, the free  $I^-$  will be fully converted and immobilized in  $[ZnI_x(OH_2)_{4-x}]^{2-x}$  ( $x = 2-4$ ) or Zn-I solvated structures.<sup>[122]</sup> The elimination of polyiodides successfully improves the cycle stability of iodine cathode, even exhibiting zero capacity fading upon long lifespans. However, previous reports indicate that the  $ZnCl_2$  salt is the only one that can formulate electrolytes with high concentrations over 10 M, which limits the practical application of this concept. Incorporation with other metal salts with high solubility could help to extend the concept to other varieties of Zn salts, such as using KOAc as a secondary salt for  $Zn(OAc)_2$ , but at the expense of low  $Zn^{2+}$  transference number. Additionally, the principles of the HCEs are not entirely clear, and further fundamental studies about the formation of ion networks in HCEs and the ion distribution near the cathode interface should be provided systematically.

Employing organic solvents as co-solvent in aqueous electrolytes can also decrease the activity of  $H_2O$  molecules and alleviate the cathode dissolution and some non-flammable organic solvents can maintain the high safety feature of the aqueous electrolyte.<sup>[123]</sup> Additionally, the existence of organic co-solvent can dramatically decrease the production cost of the HCEs.<sup>[124]</sup> Although several organic co-solvents and additives in low-concentration  $Zn^{2+}$ -ion electrolytes have had some success in redressing these issues, the efficacy is tempered by them being required in large amounts that reduce key electrolyte features such as ionic conductivity. In addition, due to the limitation of existing solutions, it is challenging to realize the simultaneous regulation of solvation structure and interfacial interaction in both anode and cathodes, resulting in inferior electrochemical stability of the full cell.

Solid-state gel catholyte has been developed to alleviate the dissolution effect of  $I_2$  cathode materials. Specifically, the gel catholyte can mitigate the dissolution of iodine and the shuttle effect of polyiodides in iodine-based cathodes because of the self-trapped polyiodides at the core-shell interface and inside the hydrophobic core of micelles.<sup>[54]</sup> The assembled AZIBs presented a high electrochemical performance, delivering the capacity of  $210 \text{ mA h g}^{-1}$  at the current density of 1 C with 94.3% retention after 500 cycles. This kind of catholyte can also be used for the design of wearable, flexible electronic devices. However, limited energy density will be obtained because additional matrixes must be used during battery operation. The strategies may be suitable for other cathodes but have not been confirmed yet.

### 3.4.2. Structural Engineering of Cathode Materials

As introduced in the previous section, the pre-intercalation strategy expands the interlayer space of cathode materials to afford regulated charge transfer kinetics. Such a strategy can also be used to stabilize the structural stability, Figure 7b. For instance, the inserted ions or molecules serve as pillars to withstand the volume change of the unit cell during continuous  $Zn^{2+}/H^+$  intercalation/de-intercalation.<sup>[63,125]</sup> This is because introducing exotic ions or molecules significantly changes the chemical bonds between host materials and the  $Zn^{2+}/H^+$ . Generally, most of the pre-inserted ions are cations (*i.e.*, metal ions and  $NH_4^+$ ), which have strong interactions with host  $O^{2-}$ ,

enhancing the stability of the crystal structure.<sup>[126]</sup> In contrast, when water and polymer molecules serve as pillars, they mainly bond with  $Zn^{2+}$  or  $H^+$  ions to regulate electrostatic interactions between the  $Zn^{2+}$  and the host  $O^{2-}$  to stabilize the cathode structure.<sup>[93b,127]</sup> A strong chemical bond is required between the polymer and  $Zn^{2+}$  or  $H^+$  ions in order to avoid the polymer being extracted out of the host materials during repeated cycling. The bond energy between the exotic polymer and  $Zn^{2+}$  or  $H^+$  ions depend on the valence state, molecule mass, and the radius size of the polymer.<sup>[90a]</sup> The quantity of the inserted polymer also has impacts on stabilizing the host structure, which should be carefully studied and optimized in the future to obtain acceptable rate capability and energy density.

In addition, another attempt has been carried out to achieve highly stable cathode materials by developing the surface coating approach. The functional coating layer could be an artificial barrier to physically separate the electrode and the aqueous electrolyte, affording minimized side reactions and mitigated dissolution.<sup>[96]</sup> This layer is also beneficial to buffering the stress originating from the volume change during the  $Zn^{2+}$  or  $Zn^{2+}/H^+$  ions intercalation/de-intercalation. Carbon materials, inorganic compounds, and organic polymers have been studied in the past few years to maintain the structural integrity of cathode materials for AZIBs.<sup>[24a,128]</sup> Carbonaceous materials are prevalent coating materials when considering their availability, excellent conductivity, capability in buffering volume change, and wide compatibility with all kinds of cathode materials. Other species involving inorganic VOOH and  $Al_2O_3$  or organic palmitic acid/polypyrrole and PEDOT: poly(styrenesulfonate) polymers have been discovered to serve as protective layers to mitigate the cathode dissolution, especially for Mn-based and V-based cathode materials.<sup>[128a,b,129]</sup> For instance, the dicyandiamide coating layer is able to suppress the disproportionation reaction of  $Mn^{3+}$  in  $MnO_2$ -based cathodes owing to the formation of  $\pi$  donor-acceptor interaction between dicyandiamide coating and  $MnO_2$ . This interaction triggers the Jahn-Teller distortion and resolves the orbital degeneracy of  $Mn^{3+}$ .<sup>[130]</sup> Noted, organic materials with small molecular structures are readily dissolved in aqueous electrolytes. Introducing macromolecular structures with functional groups will be the key for organic species as coating materials.<sup>[51,87a,131]</sup> Additionally, in situ formation of a cathode-electrolyte interface will be a promising strategy to tackle the cation dissolution issue in cathode materials, although it is challenging because both electrolyte formulas and the cathode materials should be well matched. This interface is only reported in  $Ca_2MnO_4$  and  $K_{10}[V^{IV}_6V^{V}_{18}O_{82}]$  cathode materials.<sup>[102,132]</sup> In our opinion, to be a suitable coating layer, the material is supposed to own good flexibility and robustness against repeated and vigorous volume expansion and contraction. Therefore, composite materials containing organic (*i.e.*, carbon or polymers) and inorganic species would be interesting to achieve the coating layer with enough flexibility and durability.

### 3.4.3. Composite Materials

Similar to the surface coating strategy, the formation of a composite material stabilizes the structure by buffering the volume change, Figure 7c. Porous carbonaceous materials will be the

most-studied materials to incorporate with targeted cathode materials to obtain composite materials, and most of the composite materials contain hierarchical or core-shell structures with high surface area and porous channels.<sup>[133]</sup> More importantly, composite structures with suitable pore size distribution are capable of encapsulating or absorbing the dissolved substances near the electrode, such as the dissolved polyiodides in I<sub>2</sub> cathode.<sup>[31b]</sup> To strengthen the adsorption capability, functionalized carbon materials such as introducing heteroatom, vacancies, and even organics (*i.e.*, poly(tetrahydrofuran), polyaniline, and polypyrrole) into carbon are also practical strategies.<sup>[134]</sup> Other materials with strong adsorption capacity and suitable pore size (*i.e.*, MOF, COF, or molecular sieves) could also be used.<sup>[134a]</sup> It is noted that the design of a composite structure always aims to enhance the conductive properties of Mn-based and V-based cathodes, while the effectiveness in mitigating cathode dissolution is still unknown. Much more effort should be made to develop composite materials to increase the transfer kinetics and chemical stability simultaneously.

#### 3.4.4. Separator Designs

Using a functional separator to immobilize dissolved species near the cathode surface is another useful strategy, which has been widely used in I<sub>2</sub>-based flow batteries to mitigate the shuttle problems and prevent the diffusion of I<sub>3</sub><sup>-</sup>, Figure 7d.<sup>[135]</sup> In AZIBs, a Zn-Nafion separator is recently developed to regulate the Zn<sup>2+</sup> distribution and inhibit the dissolution problems for either V<sub>2</sub>O<sub>5</sub> or MnO<sub>2</sub> cathodes.<sup>[136]</sup> In addition, MOF, cellulose, and conventional polyolefin separators can serve as separators as well, while proper modification should be made in order to meet the practical application for grid-scale energy storage in terms of performance, production cost, and synthesis procedure.<sup>[52a,137]</sup>

## 4. Strategies for Matched Zn Anode and Electrolytes

Representative fundamental science has made a significant contribution to the key knowledge and technology of AZIBs.

However, directly transferring the created knowledge and claimed high performance from academia to the industrial phase is actually difficult.<sup>[138]</sup> This is because most of the discussed knowledge and the so-called high performance are based on small-scale coin-cell configurations, where excess Zn resources, overdosed electrolytes, and low loading of cathode materials are involved. This section aims to revisit the main parameters of anode and electrolyte in AZIBs and provide some principles for AZIBs with special attention to the deployment in the industrial process.

### 4.1. Zn Anode

Many efforts are devoted to stabilizing the Zn metal anode by adopting various designs because challenges are associated with the zinc anode in alkaline solution, such as the Zn dendrite formation, H<sub>2</sub> evolution, morphology change of the Zn anode, *etc.* Among them, how to inhibit the Zn corrosion in mildly acidic aqueous electrolytes (because the ZnO formation and the growth of Zn dendrite can be suppressed) is an important topic because the corrosion will irreversibly consume both the Zn anode and the electrolyte, Figure 8a. Importantly, this corrosion issue should be further emphasized if a high utilization of Zn anode requires (referred to as high depth of discharge).<sup>[77]</sup> The role of the Zn utilization and the CE is widely ignored by current academic research, despite its great influence on the energy density of AZIBs. For example, for an identical cathode material, the energy density of the full cell can be doubled if the Zn utilization can be increased from 25% to 100%. At the same time, because of the Zn corrosion, the increase in Zn utilization will certainly cause low CE and fast cell failure under limited Zn resources. Nevertheless, most reports employ a Zn foil even more than eight times oversized with respect to the cathode. The adopted current density and capacity are far from the practical situation.<sup>[77,139]</sup> In fact, the symmetric Zn//Zn half-cell and Zn//cathode full cells should be tested with high deposition capacities in order to increase the utilization of the Zn anode. Working under large areal capacities will help judge whether the applied strategies are effective and practical. Using a thin Zn anode (*e.g.*, 10 μm) and testing under severe

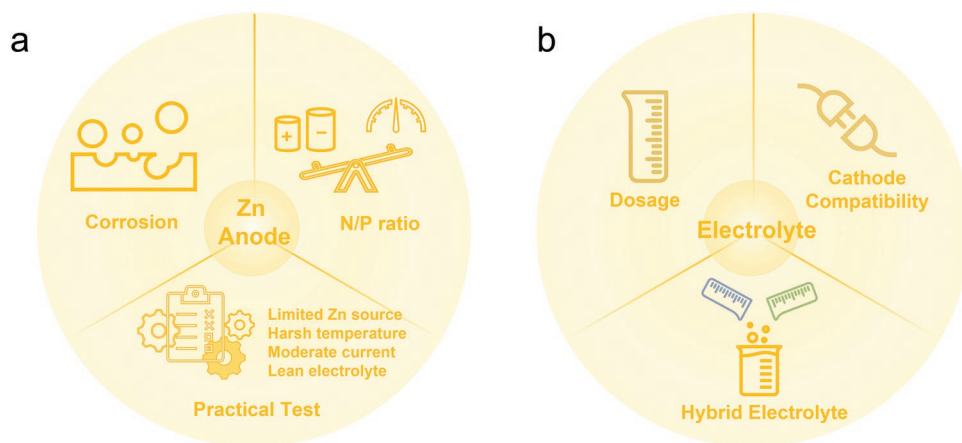


**Figure 8.** Important parameters and design principles for a) Zn anode and b) Electrolyte for practical AZIBs for large-scale application.

environments, such as high/low temperature, moderate current densities, and lean electrolyte conditions, is also recommended to mimic the realistic battery operation condition. Understanding the correlation among Zn utilization, electrolyte amount, and performance will be desperately required. Alternatively, an anode-free AZIBs would be a promising approach to unlock the energy density of Zn anode further, while the Zn corrosion and the lack of Zn-rich cathode materials with stable  $Zn^{2+}$  ions supply should be addressed.

#### 4.2. Electrolyte

In addition to the factors such as current density and Zn utilization, aqueous electrolyte is another critical reason for the reversibility of Zn anodes in a given electrochemical working window, Figure 8b. The aqueous electrolyte is also responsible for the dissolution and transfer kinetics issues of the cathode materials.  $ZnSO_4$ ,  $ZnCl_2$ , and  $Zn(OTF)_2$  are the most studied Zn salts in aqueous electrolytes for Zn-based batteries. Considering the electrolyte is usually not involved in the redox reactions, most reports focused only on the species and concentration of salts, solvent, and additives, but ignore the electrolyte dosage. In terms of energy density, the fewer the electrolyte dosage, the higher the energy density. However, an adequate amount of electrolyte must be used to sustain the normal operation of batteries. In detail, the electrolyte dosage is related to the porosity of both anode and cathode electrodes, as well as the electrolyte uptake of separators. It could be more complex for AZIBs, in which self-corrosion resulting in continuous electrolyte consumption is prevalent. As a large amount of electrolyte will sacrifice energy density, a lower dosage is recommended for AZIBs and the electrolyte dosage should be optimized and evaluated under a high Zn utilization and thick cathode electrode with high mass loading. It is very challenging to obtain the overrated battery performance under these realistic conditions, however, this will help to produce meaningful experimental results, which represent realistic ZIB working conditions.

Although electrolyte engineering is a viable strategy to improve the performance of cathode materials, there are still a shortage of systematic investigation on the compatibility issues between electrolytes and specific cathodes. Both salts and solvents are dominant components of electrolytes and dictate the primary physical properties of electrolytes and even the electrochemical performance. For AZIBs, the primary solvent is  $H_2O$ , while the potential salt could be  $ZnSO_4$ ,  $Zn(OTF)_2$ ,  $ZnCl_2$  and  $Zn(OAc)_2$ . Currently, electrolytes containing  $ZnSO_4$  and  $Zn(OTF)_2$  attract great research interests for their excellent compatibility with the Zn anode. However, it is still unclear how salts can influence the cathode materials in different electrolytes. Importantly, for Zn salts with inferior compatibility toward Zn anode may possess better compatibility with cathode materials. Maintaining good compatibility with anode and cathode is the perquisition factor toward practical application.

The adoption of non-aqueous electrolytes or hybrid electrolytes (aqueous-organic solution) for Zn batteries has drawn much attention in the past five years because electrolyte engineering is deemed to affect both the anode and cathode of

AZIBs significantly. For example, hybrid electrolytes are used to inhibit the Zn dendrite growth and byproducts formation concurrently. However, the formation mechanism of dendrite and byproduct is different and rare reports decouple the effect of electrolyte engineering on these two issues.<sup>[116e,140]</sup> Besides, organic solvents have unparalleled advantages in extreme temperature because of the wide liquid range.<sup>[141]</sup> Nevertheless, aqueous-organic solution would increase the safety concern of AZIBs, despite non-flammable organic solvents with phosphorus-containing functional groups being developed to tackle this issue. Additionally, previous work indicates that the completely non-flammable electrolyte may exhibit inferior safety performance due to its intensive reactivity, contrary to the conventional understanding.<sup>[142]</sup> For AZIBs, a major motivation is their perceived safety relative to prevalent organic LIBs, while the AZIBs using hybrid electrolytes would possibly undergo hazards such as gas evolution and safety hazards. It should be careful to choose an organic solvent and be accurate in adopting an optimal concentration. Additionally, it is challenging for an electrolyte with a single solvent capable of resolving all issues related to the anode and the cathode. Therefore, exploring new electrolytes with dual-solvents or even ternary-solvents to achieve a balanced performance of wide working windows, good compatibility with cathode and anode, and satisfying safety properties is preferred.

Additionally, tools of the atomic resolution, in situ/*operando* capability involving synchrotron/neutron diffraction, nuclear magnetic resonance, online mass spectrometry, supercomputers, and theoretical simulations, should be utilized to provide deeper insights into the reaction mechanism and develop structure-versus-electrochemical property models.

## 5. Conclusion and Prospects

AZIBs are of increasing research interest because of abundant Zn, low cost, good safety performance and high ionic conductivity.<sup>[143]</sup> So far, the lifespan and performance of Zn anode have been improved to a relatively high level.<sup>[144]</sup> Despite wide varieties, however, cathode materials still face many challenges, hindering the practical application of AZIBs. Materials used in AZIBs include, Mn-based oxides, V-based compounds, PBAs, organic compounds, layered chalcogenides and polyanions, together with conversion-type materials. Crystal structure, composition and morphology of cathodes, together with electrolyte components produces differing mechanism(s) for  $Zn^{2+}$  storage and electrochemical performance. There are six (6) energy storage mechanisms: 1)  $Zn^{2+}$  insertion/extraction, 2) conversion reactions, 3)  $H^+/Zn^{2+}$  insertion/extraction, 4) dissolution/deposition, 5) ion coordination and 6) multiple-ion insertion/extraction. The insertion/extraction chemistry is rather complex and there is a lack of a precise characterizations to determine the genuine storage mechanism including inserted ions, inserted sequence and structural change.

The cathode material also has six (6) problems to overcome before the practical commercialization: 1) dissolution of active materials, 2) parasitic byproduct formation, 3) phase change, 4) low theoretical capacity, 5) sluggish charge transfer kinetics and 6) challenge for practical application. The dissolution

problem is widely found in the cathode for AZIBs, having significant influence on the lifespan of batteries. For inorganic materials, especially the Mn-based and V-based cathodes, the dissolution primarily depends on the pH of adopted electrolytes. The molecule structure including size and functional groups is an important factor for organic compounds to resist dissolution. In contrast, halogen cathodes relying on the liquid-to-solid conversion reaction normally are soluble in the electrolyte, while the main challenge is to mitigate the diffusion of these ions toward the Zn anode. The challenge toward practical applications includes four (4) key parameters: 1) energy density, 2) safety risks, 3) cost and 4) performance. The development of cathode materials should take these requirements into consideration to achieve a good balance for commercial application.

Many modification methods have been proposed to address the problems of cathodes, including structural and morphological designs of cathodes, engineering of electrolytes and development of separators. Pre-intercalation is a multipurpose approach to concurrently stabilize the structure and increase the electrode kinetics of cathodes. A variety of chemistries including metal ions and neutral molecules can be the guest species to regulate the structure properties of cathode materials. Electrolyte engineering is a useful but feasible method to improve the stability of electrode/electrolyte interface and regulate the electrochemical storage reactions. Separator engineering can effectively mitigate the diffusion of ions from the cathode to the anode and replacing the expensive glass fiber membrane with affordable separator is a prerequisite to the practical application of AZIBs. These approaches exhibit great potentials in performance enhancement of cathodes owing to the practical effectiveness.

Future development and prospects for AZIBs include: 1) New cathodes: Prospects for development of new, and more stable cathodes, such as molybdenum-based oxides, metal phosphides, or sulfur will be important to development of AZIBs for grid-scale energy storage. Besides, polyoxovanadates (POVs) exhibit unique properties, such as the ability to construct a variety of cluster structures through the multiple valence state of V and perform rich coordination chemistry under controlled experimental conditions. A successful example of POVs is the  $K_2Zn_2V_{10}O_{28}$ , which possesses a stable skeleton structure with exceptional redox ability.<sup>[145]</sup> Compared with other cathode materials, organic cathode materials are more worthy of research owing to the flexible skeleton structure, tailored functional groups, and high theoretical capacity. However, most organic materials require complicated synthetic procedures, which hinders large-scale production. The inferior conductivity and poor crystallinity should be overcome to further optimize the performance of electrode materials for practical application. Among the potential candidates, covalent triazine frameworks would hold the promise as suitable organic electrodes for AZIBs due to the existence of stable triazine skeletons, and more exploration are expected to be provided in the future to validate these ideas. 2) Improving storage mechanism(s): Although the  $Zn^{2+}$  storage mechanisms are poorly understood, new characterization methods and advanced technologies might be practically applied to develop new understanding. For instance, in situ/operando characterization of materials, electrolyte and interface in AZIBs from the view of phase evolution, valence change,

and morphologies change. Related instruments will be in situ near ambient pressure X-ray photoelectron spectroscopy, in situ X-ray absorption spectroscopy, in situ Fourier-transform infrared spectroscopy, etc. In addition, electrochemical characterization techniques also play an important role to measure the relationship between the degradation of cathodes and the concomitant degradation of electrochemical performance. For example, in situ differential electrochemical mass spectrometry can determine mass resolved determination of gaseous reactants, reaction intermediates, and products in real-time. Considering a wide array of material candidates is required through extensive and time-consuming experimentation, machine-learning could be helpful to enable leap-step advances in the field of mechanism understanding. 3) Cathode materials optimization: Reported modification methods for cathode materials includes, pre-intercalation of “guest” species, nanostructure regulation, surface coating, introduction of defects and inorganic–organic hybrid electrodes, are more worthy of research. Mature technologies for other energy storage systems, such as those involving gradient coating, should be applied. These judiciously applied could be used to stabilize host structures. 4) Flexible batteries: AZIBs show promise for use as flexible batteries in electronic devices due to their high safety feature. Unlike traditional LIBs, AZIBs use aqueous-based electrolytes that are less prone to thermal runaway and fires, making them safer for use in flexible devices that undergo repeated bending, twisting, and other mechanical deformation. The affordable aqueous electrolyte and low-cost Zn electrodes in AZIBs make them a practical alternative for use in wearable electronic devices and even medical implanting devices. However, the development of flexible batteries for wearable electronics must focus on suitable electrolytes, as they must exhibit good biocompatibility to ensure their safety upon exposure to the human body. In this case, biocompatible hydrogel electrolytes would be a good choice. Despite this, the relatively low energy density of AZIBs compared to LIBs may require larger battery sizes to achieve a high capacity, which could be challenging in flexible devices that have limited space for batteries. Therefore, ongoing research to improve the energy density, safety, biocompatibility, and cost of AZIBs is crucial to make them an attractive option for use in flexible devices in the future. 5) Rechargeable alkaline zinc batteries: Alkaline zinc batteries offer high energy density due to the more negative redox potential of the Zn anode in alkaline electrolytes (−1.26 V vs. SHE in alkaline electrolytes, compared to −0.76 V vs. SHE in mild-acid electrolytes) when compared with mild-acid AZIBs. However, commercializing rechargeable alkaline zinc batteries faces a significant challenge due to the incompatibility between the zinc anode and alkaline electrolyte, resulting in the formation of parasitic ZnO product, dendrite formation, and electrolyte consumption. These issues can significantly affect the performance and safety of the alkaline ZIBs, limiting their commercialization. To address these issues, one of the promising approaches is to use anode protection for the Zn anode in mild-acid AZIBs, such as protective coatings or composite anodes, and optimizing the electrode structure to improve the stability of the Zn anode and reduce dendrite formation. Another promising protocol is electrolyte engineering, such as the addition of zinc salts or additives, to provide Zn anode with

good electrochemical/chemistry stability. Additionally, researchers are exploring new cathode materials that can reversibly operate in alkaline AZIBs, such as metal oxides (e.g., Ni-based oxides) and sulfides, but their compatibility with the alkaline electrolyte must be carefully evaluated to ensure optimal performance. It is concluded therefore that future prospects for aqueous zinc-based batteries will continue to grow with combined advanced characterizations and new research methods and that they will replace less cost-effective LIBs in grid-scale energy storage.

## Acknowledgements

G.L. and L.S. contributed equally to this work. This work was supported by the Australian Research Council (DP210101486 and FL210100050). H. Jin gratefully acknowledges financial support from Institute for Sustainability, Energy and Resources, The University of Adelaide, Future Making Fellowship. G. Li was supported by scholarships from the China Scholarship Council (Grant No. 202006750014).

Open access publishing facilitated by The University of Adelaide, as part of the Wiley - The University of Adelaide agreement via the Council of Australian University Librarians.

## Conflict of Interest

The authors declare no conflict of interest.

## Keywords

aqueous ZIBs, cathode materials, cathode modifications, reaction mechanisms, zinc-ion batteries

Received: February 3, 2023

Revised: March 11, 2023

Published online: April 18, 2023

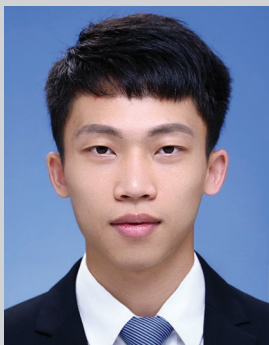
- [1] NASA, *Global Climate Change. Vital Signs of the Planet: Carbon Dioxide* **2023**. <https://climate.nasa.gov/vital-signs/carbon-dioxide/> (accessed 25 Jan 2023).
- [2] S. L. Zhang, Y. Liu, Q. N. Fan, C. F. Zhang, T. F. Zhou, K. Kalantar-Zadeh, Z. P. Guo, *Energy Environ. Sci.* **2021**, *14*, 4177.
- [3] Renewables 2021: Analysis and Forecast to 2026, International Energy Agency, [www.iea.org](http://www.iea.org). Revised version, December **2021**. (accessed 25 Jan 2023).
- [4] a) F. Yang, J. A. Yuwono, J. Hao, J. Long, L. Yuan, Y. Wang, S. Liu, Y. Fan, S. Zhao, K. Davey, Z. Guo, *Adv. Mater.* **2022**, *34*, 2206754; b) S. Liu, J. Vongsivut, Y. Wang, R. Zhang, F. Yang, S. Zhang, K. Davey, J. Mao, Z. Guo, *Angew. Chem., Int. Ed.* **2022**, *135*, e202215600; c) J. Hao, B. Li, X. Li, X. Zeng, S. Zhang, F. Yang, S. Liu, D. Li, C. Wu, Z. Guo, *Adv. Mater.* **2020**, *32*, 2003021.
- [5] a) N. Zhang, X. Chen, M. Yu, Z. Niu, F. Cheng, J. Chen, *Chem. Soc. Rev.* **2020**, *49*, 4203; b) J. Wan, R. Wang, Z. Liu, L. Zhang, F. Liang, T. Zhou, S. Zhang, L. Zhang, Q. Lu, C. Zhang, Z. Guo, *ACS Nano* **2023**, *17*, 1610.
- [6] a) F. R. McLarnon, E. J. Cairns, *J. Electrochem. Soc.* **1991**, *138*, 645; b) Y. Shen, K. Kordes, *J. Power Sources* **2000**, *87*, 162; c) C. W. Lee, K. Sathiyarayanan, S. W. Eom, M. S. Yun, *J. Power Sources* **2006**, *160*, 1436.
- [7] C. Xu, B. Li, H. Du, F. Kang, *Angew. Chem., Int. Ed.* **2012**, *51*, 933.
- [8] a) X. Zeng, J. Hao, Z. Wang, J. Mao, Z. Guo, *Energy Stor. Mater.* **2019**, *20*, 410; b) J. Hao, X. Li, S. Zhang, F. Yang, X. Zeng, S. Zhang, G. Bo, C. Wang, Z. Guo, *Adv. Funct. Mater.* **2020**, *30*, 2001263; c) J. Hao, X. Li, X. Zeng, D. Li, J. Mao, Z. Guo, *Energy Environ. Sci.* **2020**, *13*, 3917.
- [9] X. Jia, C. Liu, Z. G. Neale, J. Yang, G. Cao, *Chem. Rev.* **2020**, *120*, 7795.
- [10] a) X. Wang, Z. Zhang, B. Xi, W. Chen, Y. Jia, J. Feng, S. Xiong, *ACS Nano* **2021**, *15*, 9244; b) D. Selvakumaran, A. Pan, S. Liang, G. Cao, *J. Mater. Chem. A* **2019**, *7*, 18209; c) D. Chao, W. Zhou, C. Ye, Q. Zhang, Y. Chen, L. Gu, K. Davey, S. Z. Qiao, *Angew. Chem.* **2019**, *131*, 7905.
- [11] a) W. Shi, W. S. V. Lee, J. Xue, *ChemSusChem* **2021**, *14*, 1634; b) M. Han, L. Qin, Z. Liu, L. Zhang, X. Li, B. Lu, J. Huang, S. Liang, J. Zhou, *Mater. Today Energy* **2021**, *20*, 100626.
- [12] L. Wang, J. Zheng, *Mater. Today Adv.* **2020**, *7*, 100078.
- [13] Y. Zhang, A. Chen, J. Sun, *J. Energy Chem* **2021**, *54*, 655.
- [14] a) Y. Zhang, E. H. Ang, K. N. Dinh, K. Rui, H. Lin, J. Zhu, Q. Yan, *Mater. Chem. Front.* **2021**, *5*, 744; b) A. J. Perez, D. Batuk, M. Saubanère, G. Rousse, D. Foix, E. McCalla, E. J. Berg, R. Dugas, K. H. W. van den Bos, M.-L. Doublet, D. Gonbeau, A. M. Abakumov, G. Van Tendeloo, J.-M. Tarascon, *Chem. Mater.* **2016**, *28*, 8278.
- [15] a) R. Y. Wang, C. D. Wessells, R. A. Huggins, Y. Cui, *Nano Lett.* **2013**, *13*, 5748; b) Y. Lu, L. Wang, J. Cheng, J. B. Goodenough, *Chem. Commun.* **2012**, *48*, 6544.
- [16] Y. Li, J. Zhao, Q. Hu, T. Hao, H. Cao, X. Huang, Y. Liu, Y. Zhang, D. Lin, Y. Tang, Y. Cai, *Mater. Today Energy* **2022**, *29*, 101095.
- [17] a) L. Ma, S. Chen, C. Long, X. Li, Y. Zhao, Z. Liu, Z. Huang, B. Dong, J. A. Zapien, C. Zhi, *Adv. Energy Mater.* **2019**, *9*, 1902446; b) L. Y. Zhang, L. Chen, X. F. Zhou, Z. P. Liu, *Adv. Energy Mater.* **2015**, *5*, 1400930; c) R. Trocoli, F. La Mantia, *ChemSusChem* **2015**, *8*, 481; d) Y. Tian, M. Ju, X. Bin, Y. Luo, W. Que, *Chem. Eng. J.* **2022**, *430*, 132864.
- [18] H. Cui, L. Ma, Z. Huang, Z. Chen, C. Zhi, *SmartMat.* **2022**, *3*, 565.
- [19] T. Sun, H. J. Fan, *Curr. Opin. Electrochem.* **2021**, *30*, 100799.
- [20] X. Zhou, H. Jin, B. Y. Xia, K. Davey, Y. Zheng, S. Z. Qiao, *Adv. Mater.* **2021**, *33*, 2104341.
- [21] L. Zhang, Y. Chen, Z. Jiang, J. Chen, C. Wei, W. Wu, S. Li, Q. Xu, *Energy Environ. Mater.* **2022**.
- [22] L. Kong, M. Liu, H. Huang, Y. Xu, X. H. Bu, *Adv. Energy Mater.* **2021**, *12*, 2100172.
- [23] a) B. Liu, *Batteries* **2022**, *8*, 62; b) W. Liu, J. Hao, C. Xu, J. Mou, L. Dong, F. Jiang, Z. Kang, J. Wu, B. Jiang, F. Kang, *Chem. Commun. (Camb.)* **2017**, *53*, 6872; c) P. He, M. Yan, G. Zhang, R. Sun, L. Chen, Q. An, L. Mai, *Adv. Energy Mater.* **2017**, *7*, 1601920; d) Z. Wu, C. Lu, Y. Wang, L. Zhang, L. Jiang, W. Tian, C. Cai, Q. Gu, Z. Sun, L. Hu, *Small* **2020**, *16*, 2000698.
- [24] a) Y. Liu, J. Wang, Y. Zeng, J. Liu, X. Lu, *Small* **2020**, *16*, e1907458; b) J. Duan, K. Ji, L. Min, Y. Zhang, T. Yang, M. Chen, C. Wang, *Electrochim. Acta* **2021**, *390*, 138883; c) J. Huang, Y. Li, R. Xie, J. Li, Z. Tian, G. Chai, Y. Zhang, F. Lai, G. He, C. Liu, T. Liu, D. J. L. Brett, *J. Energy Chem.* **2021**, *58*, 147.
- [25] a) L. Wang, S. Yan, C. D. Quilty, J. Kuang, M. R. Dunkin, S. N. Ehrlich, L. Ma, K. J. Takeuchi, E. S. Takeuchi, A. C. Marschillok, *Adv. Mater. Interfaces* **2021**, *8*, 2002080; b) S. Liu, Y. Sun, J. Yang, Y. Zhang, Z. Cai, *Materials* **2022**, *15*, 5954; c) J. Meng, Z. Yang, L. Chen, H. Qin, F. Cui, Y. Jiang, X. Zeng, *Mater. Today Energy* **2020**, *15*, 100370.
- [26] a) S. Wang, S. Lu, X. Yang, X. Liu, *J. Electroanal. Chem.* **2021**, *882*, 115033; b) K. Zhang, Q. Kuang, J. Wu, N. Wen, Q. Fan, Y. Dong, Y. Zhao, *Electrochim. Acta* **2022**, *403*, 139629; c) J. Wu, J. Meng, Z. Yang, H. Chen, Y. Rong, L. Deng, Z. Fu, *J. Alloys Compd.* **2022**, *895*, 162653.
- [27] J. Yan, E. H. Ang, Y. Yang, Y. Zhang, M. Ye, W. Du, C. C. Li, *Adv. Funct. Mater.* **2021**, *31*, 2010213.

- [28] a) A. Gutierrez, N. A. Benedek, A. Manthiram, *Chem. Mater.* **2013**, *25*, 4010; b) Y.-U. Park, D.-H. Seo, H. Kim, J. Kim, S. Lee, B. Kim, K. Kang, *Adv. Funct. Mater.* **2014**, *24*, 4603.
- [29] a) P. Hu, T. Zhu, X. Wang, X. Zhou, X. Wei, X. Yao, W. Luo, C. Shi, K. A. Owusu, L. Zhou, L. Mai, *Nano Energy* **2019**, *58*, 492; b) G. Li, Z. Yang, Y. Jiang, C. Jin, W. Huang, X. Ding, Y. Huang, *Nano Energy* **2016**, *25*, 211; c) W. Li, K. Wang, S. Cheng, K. Jiang, *Energy Stor. Mater.* **2018**, *15*, 14.
- [30] F. Wan, Y. Zhang, L. Zhang, D. Liu, C. Wang, L. Song, Z. Niu, J. Chen, *Angew. Chem., Int. Ed.* **2019**, *58*, 7062.
- [31] a) L. Yan, S. Zhang, Q. Kang, X. Meng, Z. Li, T. Liu, T. Ma, Z. Lin, *Energy Stor. Mater.* **2023**, *54*, 339; b) D. Lin, Y. Li, *Adv. Mater.* **2022**, *34*, 2108856.
- [32] Q. Yang, X. Li, Z. Chen, Z. Huang, C. Zhi, *Acc. Mater. Res.* **2022**, *3*, 78.
- [33] X. Li, M. Li, Z. Huang, G. Liang, Z. Chen, Q. Yang, Q. Huang, C. Zhi, *Energy Environ. Sci.* **2021**, *14*, 407.
- [34] C. Xu, B. Li, H. Du, F. Kang, *Angew. Chem.* **2012**, *124*, 957.
- [35] H. Pan, Y. Shao, P. Yan, Y. Cheng, K. S. Han, Z. Nie, C. Wang, J. Yang, X. Li, P. Bhattacharya, K. T. Mueller, J. Liu, *Nat. Energy* **2016**, *1*, 16039.
- [36] C. Xie, T. Li, C. Deng, Y. Song, H. Zhang, X. Li, *Energy Environ. Sci.* **2020**, *13*, 135.
- [37] D. Kundu, B. D. Adams, V. Duffort, S. H. Vajargah, L. F. Nazar, *Nat. Energy* **2016**, *1*, 16119.
- [38] F. Wan, L. Zhang, X. Dai, X. Wang, Z. Niu, J. Chen, *Nat. Commun.* **2018**, *9*, 1656.
- [39] K. W. Nam, H. Kim, Y. Beldjoudi, T. W. Kwon, D. J. Kim, J. F. Stoddart, *J. Am. Chem. Soc.* **2020**, *142*, 2541.
- [40] W. S. V. Lee, T. Xiong, X. Wang, J. Xue, *Small Methods* **2021**, *5*, 2000815.
- [41] W. Li, K. Wang, K. Jiang, *Adv. Sci.* **2020**, *7*, 2000761.
- [42] V. Verma, S. Kumar, W. Manalastas, R. Satish, M. Srinivasan, *Adv. Sustain. Syst.* **2019**, *3*, 1800111.
- [43] B. Lee, C. S. Yoon, H. R. Lee, K. Y. Chung, B. W. Cho, S. H. Oh, *Sci. Rep.* **2014**, *4*, 6066.
- [44] Y. Yuan, R. Sharpe, K. He, C. Li, M. T. Saray, T. Liu, W. Yao, M. Cheng, H. Jin, S. Wang, K. Amine, R. Shahbazian-Yassar, M. S. Islam, J. Lu, *Nat. Sustain.* **2022**, *5*, 890.
- [45] S. Boyd, V. Augustyn, *Inorg. Chem. Front.* **2018**, *5*, 999.
- [46] A. M. Engstrom, F. M. Doyle, *J. Power Sources* **2013**, *228*, 120.
- [47] Y. Lu, T. Zhu, W. Bergh, M. Stefik, K. Huang, *Angew. Chem.* **2020**, *132*, 17152.
- [48] a) Z. Li, T. Liu, R. Meng, L. Gao, Y. Zou, P. Peng, Y. Shao, X. Liang, *Energy Environ. Mater.* **2020**, *4*, 111; b) G. Ni, B. Han, Q. Li, Z. Ji, B. Huang, C. Zhou, *ChemElectroChem* **2016**, *3*, 798; c) H. Y. Shi, Y. Song, Z. Qin, C. Li, D. Guo, X. X. Liu, X. Sun, *Angew. Chem., Int. Ed.* **2019**, *58*, 16057; d) W. Xu, K. Zhao, Y. Wang, *Energy Stor. Mater.* **2018**, *15*, 374.
- [49] L. Zhang, L. Chen, X. Zhou, Z. Liu, *Sci. Rep.* **2015**, *5*, 18263.
- [50] J. Cui, Z. Guo, J. Yi, X. Liu, K. Wu, P. Liang, Q. Li, Y. Liu, Y. Wang, Y. Xia, J. Zhang, *ChemSusChem* **2020**, *13*, 2160.
- [51] Q. Zhao, W. Huang, Z. Luo, L. Liu, Y. Lu, Y. Li, L. Li, J. Hu, H. Ma, J. Chen, *Sci. Adv.* **2018**, *4*, eaao1761.
- [52] a) H. Yang, Y. Qiao, Z. Chang, H. Deng, P. He, H. Zhou, *Adv. Mater.* **2020**, *32*, 2004240; b) H. Pan, B. Li, D. Mei, Z. Nie, Y. Shao, G. Li, X. S. Li, K. S. Han, K. T. Mueller, V. Sprenkle, J. Liu, *ACS Energy Lett.* **2017**, *2*, 2674.
- [53] S. J. Zhang, J. Hao, H. Li, P. F. Zhang, Z. W. Yin, Y. Y. Li, B. Zhang, Z. Lin, S. Z. Qiao, *Adv. Mater.* **2022**, *34*, 2201716.
- [54] K. K. Sonigara, J. Zhao, H. K. Machhi, G. Cui, S. S. Soni, *Adv. Energy Mater.* **2020**, *10*, 2001997.
- [55] Z. Zhu, T. Jiang, M. Ali, Y. Meng, Y. Jin, Y. Cui, W. Chen, *Chem. Rev.* **2022**, *122*, 16610.
- [56] a) P. Oberholzer, E. Tervoort, A. Bouzid, A. Pasquarello, D. Kundu, *ACS Appl. Mater. Interfaces* **2019**, *11*, 674; b) C. Xia, J. Guo, Y. Lei, H. Liang, C. Zhao, H. N. Alshareef, *Adv. Mater.* **2018**, *30*, 1705580; c) L. Zhang, I. A. Rodríguez-Pérez, H. Jiang, C. Zhang, D. P. Leonard, Q. Guo, W. Wang, S. Han, L. Wang, X. Ji, *Adv. Funct. Mater.* **2019**, *29*, 1902653; d) M. Li, Z. Li, X. Wang, J. Meng, X. Liu, B. Wu, C. Han, L. Mai, *Energy Environ. Sci.* **2021**, *14*, 3796.
- [57] Q. Pang, H. Zhao, R. Lian, Q. Fu, Y. Wei, A. Sarapulova, J. Sun, C. Wang, G. Chen, H. Ehrenberg, *J. Mater. Chem. A* **2020**, *8*, 9567.
- [58] a) D. Kundu, S. Hosseini Vajargah, L. Wan, B. Adams, D. Prendergast, L. F. Nazar, *Energy Environ. Sci.* **2018**, *11*, 881; b) B. Lee, H. R. Seo, H. R. Lee, C. S. Yoon, J. H. Kim, K. Y. Chung, B. W. Cho, S. H. Oh, *ChemSusChem* **2016**, *9*, 2948; c) V. Verma, S. Kumar, W. Manalastas, M. Srinivasan, *ACS Energy Lett.* **2021**, *6*, 1773.
- [59] a) L. Zhang, I. A. Rodríguez-Pérez, H. Jiang, C. Zhang, D. P. Leonard, Q. Guo, W. Wang, S. Han, L. Wang, X. Ji, *Adv. Funct. Mater.* **2019**, *29*, 1902653; b) C. Xia, J. Guo, Y. Lei, H. Liang, C. Zhao, H. N. Alshareef, *Adv. Mater.* **2018**, *30*, 1705580; c) F. Liu, Z. Chen, G. Fang, Z. Wang, Y. Cai, B. Tang, J. Zhou, S. Liang, *Nanomicro Lett.* **2019**, *11*, 25.
- [60] a) T. Zhang, Y. Tang, S. Guo, X. Cao, A. Pan, G. Fang, J. Zhou, S. Liang, *Energy Environ. Sci.* **2020**, *13*, 4625; b) L. Droguet, A. Grimaud, O. Fontaine, J. M. Tarascon, *Adv. Energy Mater.* **2020**, *10*, 2002440.
- [61] I. Aguilar, P. Lemaire, N. Ayouni, E. Bendadesse, A. V. Morozov, O. Sel, V. Balland, B. Limoges, A. M. Abakumov, E. Raymundo-Piñero, A. Slodczyk, A. Canizarès, D. Larcher, J.-M. Tarascon, *Energy Stor. Mater.* **2022**, *53*, 238.
- [62] M. Shi, B. Wang, Y. Shen, J. Jiang, W. Zhu, Y. Su, M. Narayanasamy, S. Angaiah, C. Yan, Q. Peng, *Chem. Eng. J.* **2020**, *399*, 125627.
- [63] W. Zhang, C. Zuo, C. Tang, W. Tang, B. Lan, X. Fu, S. Dong, P. Luo, *Energy Technol.* **2020**, *9*, 2000789.
- [64] J. Ding, H. Gao, D. Ji, K. Zhao, S. Wang, F. Cheng, *J. Mater. Chem. A* **2021**, *9*, 5258.
- [65] B. Yong, D. Ma, Y. Wang, H. Mi, C. He, P. Zhang, *Adv. Energy Mater.* **2020**, *10*, 2002354.
- [66] a) J. Huang, Y. Li, R. Xie, J. Li, Z. Tian, G. Chai, Y. Zhang, F. Lai, G. He, C. Liu, T. Liu, D. J. L. Brett, *J. Energy Chem.* **2021**, *58*, 147; b) Y. Wang, J. Yin, J. Zhu, *Chin. J. Chem.* **2022**, *40*, 973.
- [67] C. Yuan, Y. Zhang, Y. Pan, X. Liu, G. Wang, D. Cao, *Electrochim. Acta* **2014**, *116*, 404.
- [68] C. Han, J. Zhu, C. Zhi, H. Li, *J. Mater. Chem. A* **2020**, *8*, 15479.
- [69] a) Z. Zhang, W. Li, Y. Shen, R. Wang, H. Li, M. Zhou, W. Wang, K. Wang, K. Jiang, *J. Energy Storage* **2022**, *45*, 103729; b) X. Geng, Y. Jiao, Y. Han, A. Mukhopadhyay, L. Yang, H. Zhu, *Adv. Funct. Mater.* **2017**, *27*, 1702998; c) M. Przeźniak-Welenc, N. A. Szreder, A. Winiarski, M. Łapiński, B. Kościńska, R. J. Barczyński, M. Gazda, W. Sadowski, *Phys. Status Solidi* **2015**, *252*, 2111.
- [70] M. Ue, K. Sakaushi, K. Uosaki, *Mater. Horiz.* **2020**, *7*, 1937.
- [71] Z. Yang, J. Zhang, M. C. Kintner-Meyer, X. Lu, D. Choi, J. P. Lemmon, J. Liu, *Chem. Rev.* **2011**, *111*, 3577.
- [72] L. Sun, G. Li, S. Zhang, S. Liu, J. Yuwono, J. Mao, Z. Guo, *Sci. China Chem.* **2022**, *65*.
- [73] T. M. Gür, *Energy Environ. Sci.* **2018**, *11*, 2696.
- [74] S. Chu, A. Majumdar, *Nature* **2012**, *488*, 294.
- [75] B. Tang, L. Shan, S. Liang, J. Zhou, *Energy Environ. Sci.* **2019**, *12*, 3288.
- [76] a) C. Li, X. Zhang, W. He, G. Xu, R. Sun, *J. Power Sources* **2020**, *449*, 227596; b) A. N. Laboratory, *Battery Performance and Cost Modeling for Electric Drive Vehicles*, Argonne National Laboratory, <https://publications.anl.gov/anlpubs/2022/07/176234.pdf>.
- [77] G. Zampardi, F. La Mantia, *Nat. Commun.* **2022**, *13*, 687.
- [78] B. Wu, B. Guo, Y. Chen, Y. Mu, H. Qu, M. Lin, J. Bai, T. Zhao, L. Zeng, *Energy Stor. Mater.* **2023**, *54*, 75.
- [79] Z. Wu, F. Ye, Q. Liu, R. Pang, Y. Liu, L. Jiang, Z. Tang, L. Hu, *Adv. Energy Mater.* **2022**, *12*, 2200654.

- [80] a) G. H. Lee, V. W. h. Lau, W. Yang, Y. M. Kang, *Adv. Energy Mater.* **2021**, *11*, 2003227; b) X. Cao, H. Li, Y. Qiao, X. Li, M. Jia, J. Cabana, H. Zhou, *Adv. Energy Mater.* **2020**, *10*, 1903785.
- [81] a) W. Chen, G. Li, A. Pei, Y. Li, L. Liao, H. Wang, J. Wan, Z. Liang, G. Chen, H. Zhang, J. Wang, Y. Cui, *Nat. Energy* **2018**, *3*, 428; b) D. Chao, W. Zhou, C. Ye, Q. Zhang, Y. Chen, L. Gu, K. Davey, S. Z. Qiao, *Angew. Chem., Int. Ed.* **2019**, *58*, 7823; c) X. Zeng, J. Liu, J. Mao, J. Hao, Z. Wang, S. Zhou, C. D. Ling, Z. Guo, *Adv. Energy Mater.* **2020**, *10*, 1904163.
- [82] a) A. Z. Yazdi, J. Zhi, M. Zhou, T. K. A. Hoang, M. Han, L. Ma, T. Zheng, D. Li, P. Chen, *ACS Appl. Energy Mater.* **2021**, *4*, 7759; b) H. B. Zhao, C. J. Hu, H. W. Cheng, J. H. Fang, Y. P. Xie, W. Y. Fang, T. N. Doan, T. K. Hoang, J. Q. Xu, P. Chen, *Sci. Rep.* **2016**, *6*, 25809; c) Q. Li, K. Ma, C. Hong, G. Yang, C. Wang, *Sci. China Mater.* **2021**, *64*, 1386.
- [83] a) L. Suo, O. Borodin, T. Gao, M. Olguin, J. Ho, X. Fan, C. Luo, C. Wang, K. Xu, *Science* **2015**, *350*, 938; b) R. S. Kuhnel, D. Reber, A. Remhof, R. Figi, D. Bleiner, C. Battaglia, *Chem. Commun.* **2016**, *52*, 10435.
- [84] a) T. Yokoji, H. Matsubara, M. Satoh, *J. Mater. Chem. A* **2014**, *2*, 19347; b) Y. Liang, P. Zhang, S. Yang, Z. Tao, J. Chen, *Adv. Energy Mater.* **2013**, *3*, 600; c) Y. Lu, Q. Zhang, L. Li, Z. Niu, J. Chen, *Chem* **2018**, *4*, 2786.
- [85] a) D. Wu, Z. Xie, Z. Zhou, P. Shen, Z. Chen, *J. Mater. Chem. A* **2015**, *3*, 19137; b) H. Zhang, Y. Fang, F. Yang, X. Liu, X. Lu, *Energy Environ. Sci.* **2020**, *13*, 2515.
- [86] a) H. Cui, T. Wang, Z. Huang, G. Liang, Z. Chen, A. Chen, D. Wang, Q. Yang, H. Hong, J. Fan, C. Zhi, *Angew. Chem.* **2022**, *134*, e202203453; b) Y. Luo, F. Zheng, L. Liu, K. Lei, X. Hou, G. Xu, H. Meng, J. Shi, F. Li, *ChemSusChem* **2020**, *13*, 2239.
- [87] a) Z. Tie, Z. Niu, *Angew. Chem., Int. Ed.* **2020**, *59*, 21293; b) Z. Tie, L. Liu, S. Deng, D. Zhao, Z. Niu, *Angew. Chem., Int. Ed.* **2020**, *59*, 4920.
- [88] P. He, M. Yan, X. Liao, Y. Luo, L. Mai, C.-W. Nan, *Energy Stor. Mater.* **2020**, *29*, 113.
- [89] a) M. Liao, J. Wang, L. Ye, H. Sun, Y. Wen, C. Wang, X. Sun, B. Wang, H. Peng, *Angew. Chem., Int. Ed.* **2020**, *59*, 2273; b) Z. Qi, T. Xiong, T. Chen, W. Shi, M. Zhang, Z. W. J. Ang, H. Fan, H. Xiao, W. S. V. Lee, J. Xue, *J. Alloys Compd.* **2021**, *870*, 159403; c) Y. Zhang, L. Zhao, A. Chen, J. Sun, *Fundam. Res.* **2021**, *1*, 418.
- [90] a) B. Tang, G. Fang, J. Zhou, L. Wang, Y. Lei, C. Wang, T. Lin, Y. Tang, S. Liang, *Nano Energy* **2018**, *51*, 579; b) L. Shan, Y. Yang, W. Zhang, H. Chen, G. Fang, J. Zhou, S. Liang, *Energy Stor. Mater.* **2019**, *18*, 10; c) P. Hu, T. Zhu, X. Wang, X. Wei, M. Yan, J. Li, W. Luo, W. Yang, W. Zhang, L. Zhou, Z. Zhou, L. Mai, *Nano Lett.* **2018**, *18*, 1758; d) K. Zhu, T. Wu, K. Huang, *Adv. Energy Mater.* **2019**, *9*, 1901968; e) C. Xia, J. Guo, P. Li, X. Zhang, H. N. Alshareef, *Angew. Chem., Int. Ed.* **2018**, *57*, 3943.
- [91] Y. Yang, Y. Tang, S. Liang, Z. Wu, G. Fang, X. Cao, C. Wang, T. Lin, A. Pan, J. Zhou, *Nano Energy* **2019**, *61*, 617.
- [92] a) Z. Chen, K. Leng, X. Zhao, S. Malkhandi, W. Tang, B. Tian, L. Dong, L. Zheng, M. Lin, B. S. Yeo, K. P. Loh, *Nat. Commun.* **2017**, *8*, 14548; b) S. Lemaux, A. S. Golub, P. Gressier, G. Ouvrard, *J. Solid State Chem.* **1999**, *147*, 336; c) J. P. Motter, K. J. Koski, Y. Cui, *Chem. Mater.* **2014**, *26*, 2313.
- [93] a) D. Bin, W. Huo, Y. Yuan, J. Huang, Y. Liu, Y. Zhang, F. Dong, Y. Wang, Y. Xia, *Chem* **2020**, *6*, 968; b) J. Huang, Z. Wang, M. Hou, X. Dong, Y. Liu, Y. Wang, Y. Xia, *Nat. Commun.* **2018**, *9*, 2906.
- [94] J. Long, J. Gu, Z. Yang, J. Mao, J. Hao, Z. Chen, Z. Guo, *J. Mater. Chem. A* **2019**, *7*, 17854.
- [95] Y. Zhang, S. Deng, M. Luo, G. Pan, Y. Zeng, X. Lu, C. Ai, Q. Liu, Q. Xiong, X. Wang, X. Xia, J. Tu, *Small* **2019**, *15*, 1905452.
- [96] M. Du, Z. Miao, H. Li, Y. Sang, H. Liu, S. Wang, *J. Mater. Chem. A* **2021**, *9*, 19245.
- [97] a) J. Li, N. Luo, F. Wan, S. Zhao, Z. Li, W. Li, J. Guo, P. R. Shearing, D. J. L. Brett, C. J. Carmalt, G. Chai, G. He, I. P. Parkin, *Nanoscale* **2020**, *12*, 20638; b) Z. Li, Y. Ren, L. Mo, C. Liu, K. Hsu, Y. Ding, X. Zhang, X. Li, L. Hu, D. Ji, G. Cao, *ACS Nano* **2020**, *14*, 5581.
- [98] a) K. Yao, Z. Xu, J. Huang, M. Ma, L. Fu, X. Shen, J. Li, M. Fu, *Small* **2019**, *15*, e1805405; b) Y. Li, R. Zhang, W. Zhou, X. Wu, H. Zhang, J. Zhang, *ACS Nano* **2019**, *13*, 5533.
- [99] a) D. Xu, H. Wang, F. Li, Z. Guan, R. Wang, B. He, Y. Gong, X. Hu, *Adv. Mater. Interfaces* **2019**, *6*, 1801506; b) C. Guo, S. Tian, B. Chen, H. Liu, J. Li, *Mater. Lett.* **2020**, *262*, 127180.
- [100] Y. Shen, Z. Li, Z. Cui, K. Zhang, R. Zou, F. Yang, K. Xu, *J. Mater. Chem. A* **2020**, *8*, 21044.
- [101] T. Zhai, L. Wan, S. Sun, Q. Chen, J. Sun, Q. Xia, H. Xia, *Adv. Mater.* **2017**, *29*, 1604167.
- [102] S. Guo, S. Liang, B. Zhang, G. Fang, D. Ma, J. Zhou, *ACS Nano* **2019**, *13*, 13456.
- [103] a) C. Tan, H. Zhang, *Chem. Soc. Rev.* **2015**, *44*, 2713; b) Q. Lu, Y. Yu, Q. Ma, B. Chen, H. Zhang, *Adv. Mater.* **2016**, *28*, 1917; c) C. Guo, S. Tian, B. Chen, H. Liu, J. Li, *Mater. Lett.* **2020**, *262*, 127180.
- [104] a) B. Wu, G. Zhang, M. Yan, T. Xiong, P. He, L. He, X. Xu, L. Mai, *Small* **2018**, *14*, 1703850; b) S. Khamsanga, R. Pornprasertsuk, T. Yonezawa, A. A. Mohamad, S. Kheawhom, *Sci. Rep.* **2019**, *9*, 8441.
- [105] C. Zhu, R. E. Usiskin, Y. Yu, J. Maier, *Science* **2017**, *358*, 6369.
- [106] a) H. Luo, B. Wang, F. Wang, J. Yang, F. Wu, Y. Ning, Y. Zhou, D. Wang, H. Liu, S. Dou, *ACS Nano* **2020**, *14*, 7328; b) P. Liu, W. Liu, Y. Huang, P. Li, J. Yan, K. Liu, *Energy Stor. Mater.* **2020**, *25*, 858; c) J. N. Tiwari, R. N. Tiwari, K. S. Kim, *Prog. Mater. Sci.* **2012**, *57*, 724.
- [107] a) L. Jiang, Z. Wu, Y. Wang, W. Tian, Z. Yi, C. Cai, Y. Jiang, L. Hu, *ACS Nano* **2019**, *13*, 10376; b) Z. Cao, L. Wang, H. Zhang, X. Zhang, J. Liao, J. Dong, J. Shi, P. Zhuang, Y. Cao, M. Ye, J. Shen, P. M. Ajayan, *Adv. Funct. Mater.* **2020**, *30*, 2000472; c) X. Chen, L. Wang, H. Li, F. Cheng, J. Chen, *J. Energy Chem.* **2019**, *38*, 20; d) W. Zhou, J. Chen, M. Chen, X. Xu, Q. Tian, J. Xu, C. P. Wong, *RSC Adv.* **2019**, *9*, 30556; e) P. Jing, W. Wei, W. Luo, X. Li, F. Xu, H. Li, M. Wei, D. Yu, Q. Zhu, G. Liu, *Inorg. Chem. Commun.* **2020**, *117*, 107953; f) X. Wang, L. Ma, P. Zhang, H. Wang, S. Li, S. Ji, Z. Wen, J. Sun, *Appl. Surf. Sci.* **2020**, *502*, 144207; g) L. Chen, Z. Yang, F. Cui, J. Meng, H. Chen, X. Zeng, *Appl. Surf. Sci.* **2020**, *507*, 145137; h) H. Ren, J. Zhao, L. Yang, Q. Liang, S. Madhavi, Q. Yan, *Nano Res.* **2019**, *12*, 1347.
- [108] a) H. Jin, X. Liu, A. Vasileff, Y. Jiao, Y. Zhao, Y. Zheng, S. Z. Qiao, *ACS Nano* **2018**, *12*, 12761; b) H. Jin, T. Song, U. Paik, S.-Z. Qiao, *Acc. Mater. Res.* **2021**, *2*, 559; c) H. Jin, H. Yu, H. Li, K. Davey, T. Song, U. Paik, S. Z. Qiao, *Angew. Chem., Int. Ed.* **2022**, *61*, e202203850.
- [109] S. Zhang, Y. Zheng, X. Huang, J. Hong, B. Cao, J. Hao, Q. Fan, T. Zhou, Z. Guo, *Adv. Energy Mater.* **2019**, *9*, 1900081.
- [110] a) J. Liu, T. Ma, M. Zhou, S. Liu, J. Xiao, Z. Tao, J. Chen, *Inorg. Chem. Front.* **2019**, *6*, 731; b) B. Zhang, D. Wang, Y. Hou, S. Yang, X. H. Yang, J. H. Zhong, J. Liu, H. F. Wang, P. Hu, H. J. Zhao, H. G. Yang, *Sci. Rep.* **2013**, *3*, 1836; c) M. Wang, A. M. Anghel, B. Marsan, N. L. Cevey Ha, N. Pootrakulchote, S. M. Zakeeruddin, M. Gratzel, *J. Am. Chem. Soc.* **2009**, *131*, 15976.
- [111] a) F. Wang, Z. Liu, C. Yang, H. Zhong, G. Nam, P. Zhang, R. Dong, Y. Wu, J. Cho, J. Zhang, X. Feng, *Adv. Mater.* **2020**, *32*, 1905361; b) L. Ma, Y. Ying, S. Chen, Z. Huang, X. Li, H. Huang, C. Zhi, *Angew. Chem., Int. Ed.* **2021**, *60*, 3791.
- [112] S. Zhang, L. Sun, Q. Fan, F. Zhang, Z. Wang, J. Zou, S. Zhao, J. Mao, Z. Guo, *Nano Research Energy* **2022**, *1*, e9120001.
- [113] J. Liu, P. Xu, J. Liang, H. Liu, W. Peng, Y. Li, F. Zhang, X. Fan, *Chem. Eng. J.* **2020**, *389*, 124405.
- [114] J. Ding, Z. Du, B. Li, L. Wang, S. Wang, Y. Gong, S. Yang, *Adv. Mater.* **2019**, *31*, 1904369.



- [115] a) G. Dawut, Y. Lu, L. Miao, J. Chen, *Inorg. Chem. Front.* **2018**, 5, 1391; b) J. Xie, F. Yu, J. Zhao, W. Guo, H.-L. Zhang, G. Cui, Q. Zhang, *Energy Stor. Mater.* **2020**, 33, 283.
- [116] a) Y. Wang, Z. Wang, F. Yang, S. Liu, S. Zhang, J. Mao, Z. Guo, *Small* **2022**, 18, e2107033; b) J. Mao, C. Wang, Y. Lyu, R. Zhang, Y. Wang, S. Liu, Z. Wang, S. Zhang, Z. Guo, *J. Mater. Chem. A* **2022**, 10, 19090; c) Q. Fan, J. Jiang, S. Zhang, T. Zhou, W. K. Pang, Q. Gu, H. Liu, Z. Guo, J. Wang, *Adv. Energy Mater.* **2021**, 11, 2100957; d) S. Zhang, J. Hong, X. Zeng, J. Hao, Y. Zheng, Q. Fan, W. K. Pang, C. Zhang, T. Zhou, Z. Guo, *Adv. Funct. Mater.* **2021**, 31, 2101676; e) X. Zeng, J. Mao, J. Hao, J. Liu, S. Liu, Z. Wang, Y. Wang, S. Zhang, T. Zheng, J. Liu, P. Rao, Z. Guo, *Adv. Mater.* **2021**, 33, 2007416.
- [117] a) S. N. Bhattachar, L. A. Deschenes, J. A. Wesley, *Drug Discov. Today* **2006**, 11, 1012; b) A. T. Serajuddin, P. C. Sheen, M. A. Augustine, *J. Pharm. Pharmacol.* **1987**, 39, 587.
- [118] Y. Lu, H. Zhang, H. Liu, Z. Nie, F. Xu, Y. Zhao, J. Zhu, W. Huang, *Nano Lett.* **2021**, 21, 9651.
- [119] a) M. Han, J. Huang, S. Liang, L. Shan, X. Xie, Z. Yi, Y. Wang, S. Guo, J. Zhou, *iScience* **2020**, 23, 100797; b) J. Wang, J.-G. Wang, H. Liu, C. Wei, F. Kang, *J. Mater. Chem. A* **2019**, 7, 13727; c) N. Liu, X. Wu, Y. Yin, A. Chen, C. Zhao, Z. Guo, L. Fan, N. Zhang, *ACS Appl. Mater. Interfaces* **2020**, 12, 28199.
- [120] S. Liu, J. He, D.-s. Liu, M. Ye, Y. Zhang, Y. Qin, C. C. Li, *Energy Stor. Mater.* **2022**, 49, 93.
- [121] J. Duan, K. Ji, L. Min, Y. Zhang, T. Yang, M. Chen, C. Wang, *Electrochim. Acta* **2021**, 390, 138883.
- [122] a) J. J. Hong, L. Zhu, C. Chen, L. Tang, H. Jiang, B. Jin, T. C. Gallagher, Q. Guo, C. Fang, X. Ji, *Angew. Chem., Int. Ed.* **2019**, 58, 15910; b) W. Wu, C. Li, Z. Wang, H.-Y. Shi, Y. Song, X.-X. Liu, X. Sun, *Chem. Eng. J.* **2022**, 428, 131283.
- [123] a) D. S. Liu, Y. Zhang, S. Liu, L. Wei, S. You, D. Chen, M. Ye, Y. Yang, X. Rui, Y. Qin, C. C. Li, *Adv. Funct. Mater.* **2022**, 32, 2111714; b) Y. Sun, Z. Xu, X. Xu, Y. Nie, J. Tu, A. Zhou, J. Zhang, L. Qiu, F. Chen, J. Xie, T. Zhu, X. Zhao, *Energy Stor. Mater.* **2022**, 48, 192; c) B. Kakoty, R. Vengarathody, S. Mukherji, V. Ahuja, A. Joseph, C. Narayana, S. Balasubramanian, P. Senguttuvan, *J. Mater. Chem. A* **2022**, 10, 12597.
- [124] S. Liu, J. Mao, W. K. Pang, J. Vongsivut, X. Zeng, L. Thomsen, Y. Wang, J. Liu, D. Li, Z. Guo, *Adv. Funct. Mater.* **2021**, 31, 2104281.
- [125] a) P. He, S. Chen, *Electrochem. Sci. Adv.* **2021**, 2, e2100090; b) J. Yang, G. Yao, Z. Li, Y. Zhang, L. Wei, H. Niu, Q. Chen, F. Zheng, *Small* **2023**, 19, e2205544.
- [126] a) L. Chen, Q. An, L. Mai, *Adv. Mater. Interfaces* **2019**, 6, 1900387; b) S. Chen, Y. Zhang, H. Geng, Y. Yang, X. Rui, C. C. Li, *J. Power Sources* **2019**, 441, 227192; c) T. Sun, S. Zheng, Q. Nian, Z. Tao, *Small* **2022**, 18, e2107115.
- [127] a) S. Liu, H. Zhu, B. Zhang, G. Li, H. Zhu, Y. Ren, H. Geng, Y. Yang, Q. Liu, C. C. Li, *Adv. Mater.* **2020**, 32, 2001113; b) M. Yan, P. He, Y. Chen, S. Wang, Q. Wei, K. Zhao, X. Xu, Q. An, Y. Shuang, Y. Shao, K. T. Mueller, L. Mai, J. Liu, J. Yang, *Adv. Mater.* **2018**, 30, 1703725.
- [128] a) Y. Fu, Q. Wei, G. Zhang, X. Wang, J. Zhang, Y. Hu, D. Wang, L. Zuin, T. Zhou, Y. Wu, S. Sun, *Adv. Energy Mater.* **2018**, 8, 1801445; b) X. Pu, T. Song, L. Tang, Y. Tao, T. Cao, Q. Xu, H. Liu, Y. Wang, Y. Xia, *J. Power Sources* **2019**, 437, 226917; c) X. Yue, H. Liu, P. Liu, *Chem. Commun.* **2019**, 55, 1647.
- [129] a) Y. Zhao, L. Ma, Y. Zhu, P. Qin, H. Li, F. Mo, D. Wang, G. Liang, Q. Yang, W. Liu, C. Zhi, *ACS Nano* **2019**, 13, 7270; b) X. Xiao, H. Zhang, W. Wu, C. Wang, S. Wu, G. Zhong, K. Xu, J. Zeng, W. Su, X. Lu, *Part. Part. Syst. Character.* **2019**, 36, 1900183.
- [130] J. Heo, S. Chong, S. Kim, R. Kim, K. Shin, J. Kim, H. T. Kim, *Batteries Supercaps* **2021**, 4, 1881.
- [131] Y. Zhao, Y. Wang, Z. Zhao, J. Zhao, T. Xin, N. Wang, J. Liu, *Energy Stor. Mater.* **2020**, 28, 64.
- [132] K. Yang, Y. Hu, T. Zhang, B. Wang, J. Qin, N. Li, Z. Zhao, J. Zhao, D. Chao, *Adv. Energy Mater.* **2022**, 12, 2202671.
- [133] a) H. Wang, S. Zhang, C. Deng, *ACS Appl. Mater. Interfaces* **2019**, 11, 35796; b) G. Xu, X. Liu, S. Huang, L. Li, X. Wei, J. Cao, L. Yang, P. K. Chu, *ACS Appl. Mater. Interfaces* **2020**, 12, 706; c) S. Gull, S.-C. Huang, C.-S. Ni, S.-F. Liu, W.-H. Lin, H.-Y. Chen, *J. Mater. Chem. A* **2022**, 10, 14540; d) C. Li, C. Liu, Y. Wang, Y. Lu, L. Zhu, T. Sun, *Energy Stor. Mater.* **2022**, 49, 144.
- [134] a) T. Yamamoto, M. Hishinuma, H. Sugimoto, A. Yamamoto, H. Sukawa, *J. Electroanal. Chem.* **1985**, 194, 197; b) W. Wu, C. Li, Z. Wang, H.-Y. Shi, Y. Song, X.-X. Liu, X. Sun, *Chem. Eng. J.* **2022**, 428, 131283; c) D. Lin, D. Rao, S. Chiovoloni, S. Wang, J. Q. Lu, Y. Li, *Nano Lett.* **2021**, 21, 4129.
- [135] a) T. Yamamoto, M. Hishinuma, A. Yamamoto, *Inorg. Chim. Acta* **1984**, 86, L47; b) B. Li, Z. Nie, M. Vijayakumar, G. Li, J. Liu, V. Sprenkle, W. Wang, *Nat. Commun.* **2015**, 6, 6303.
- [136] B. Wu, Y. Wu, Z. Lu, J. Zhang, N. Han, Y. Wang, X.-m. Li, M. Lin, L. Zeng, *J. Mater. Chem. A* **2021**, 9, 4734.
- [137] J. Wu, Q. Dai, H. Zhang, X. Li, *Energy Stor. Mater.* **2021**, 35, 687.
- [138] a) J. Li, C. Arbizzani, S. Kjelstrup, J. Xiao, Y.-y. Xia, Y. Yu, Y. Yang, I. Belharouak, T. Zawodzinski, S.-T. Myung, R. Raccichini, S. Passerini, *J. Power Sources* **2020**, 452, 227824; b) A. K. Stephan, *Joule* **2021**, 5, 1; c) Y.-K. Sun, *ACS Energy Lett.* **2021**, 6, 2187.
- [139] Y. Li, B. Liu, J. Ding, X. Han, Y. Deng, T. Wu, K. Amine, W. Hu, C. Zhong, J. Lu, *Batteries Supercaps* **2020**, 4, 60.
- [140] a) Y. Geng, L. Pan, Z. Peng, Z. Sun, H. Lin, C. Mao, L. Wang, L. Dai, H. Liu, K. Pan, X. Wu, Q. Zhang, Z. He, *Energy Stor. Mater.* **2022**, 51, 733; b) X. Zeng, K. Xie, S. Liu, S. Zhang, J. Hao, J. Liu, W. K. Pang, J. Liu, P. Rao, Q. Wang, J. Mao, Z. Guo, *Energy Environ. Sci.* **2021**, 14, 5947.
- [141] a) S. Liu, R. Zhang, J. Mao, Y. Zhao, Q. Cai, Z. Guo, *Sci. Adv.* **2022**, 8, eabn5097; b) J. Hao, L. Yuan, C. Ye, D. Chao, K. Davey, Z. Guo, S. Z. Qiao, *Angew. Chem., Int. Ed.* **2021**, 60, 7366.
- [142] H. Jia, Z. Yang, Y. Xu, P. Gao, L. Zhong, D. J. Kautz, D. Wu, B. Fliegler, M. H. Engelhard, B. E. Matthews, B. Broekhuis, X. Cao, J. Fan, C. Wang, F. Lin, W. Xu, *Adv. Energy Mater.* **2023**, 13, 2203144.
- [143] D. Wu, X. Li, X. Liu, J. Yi, P. Acevedo-Peña, E. Reguera, K. Zhu, D. Bin, N. Melzack, R. G. A. Wills, J. Huang, X. Wang, X. Lin, D. Yu, J. Ma, *J. Phys. Energy* **2022**, 4, 041501.
- [144] a) F. Tao, Y. Liu, X. Ren, J. Wang, Y. Zhou, Y. Miao, F. Ren, S. Wei, J. Ma, *J. Energy Chem.* **2022**, 66, 397; b) C. Liu, Z. Luo, W. Deng, W. Wei, L. Chen, A. Pan, J. Ma, C. Wang, L. Zhu, L. Xie, X.-Y. Cao, J. Hu, G. Zou, H. Hou, X. Ji, *ACS Energy Lett.* **2021**, 6, 675.
- [145] T. Zhou, L. Zhu, L. Xie, Q. Han, X. Yang, X. Cao, J. Ma, *Small* **2022**, 18, 2107102.



**Guanjie Li** received his master's degree from the South China Normal University in 2020. He is currently a PhD candidate at University of Adelaide, under the supervision of Prof. Zaiping Guo. His current research interests focus on the design of functional electrolytes for zinc-ion batteries, and the properties of cathode/electrolyte interface.



**Liang Sun** is currently a PhD candidate in the University of Adelaide, Adelaide, Australia. His research focuses on the design and fabrication of novel materials in new-generation energy storage and conversion, such as Li/Na/K-CO<sub>2</sub> batteries.



**Zaiping Guo** is an ARC Australian Laureate Fellow at the School of Chemical Engineering & Advanced Materials, The University of Adelaide. She received her PhD degree in Materials Engineering from the University of Wollongong in 2003. Before joining the University of Adelaide, she was a Distinguished Professor at the University of Wollongong. Her research focuses on the design and application of electrode and electrolyte materials for energy storage and conversion, including rechargeable batteries, hydrogen storage, and fuel cells.